### 7.1.2 Current Applications

Almost one-half million buildings in the U.S. were constructed or retrofitted with passive features in the twenty years after 1980. Passive heating applications are primarily in single-family dwellings and secondarily in small commercial buildings. Daylighting features, which reduce lighting loads and the associated cooling loads, are usually more appropriate for large office buildings.

A typical passive heating design in a favorable climate might supply up to one-third of a home's original load at a cost of $5 to $10 per million Btu (1.7¢ to 3.5¢ per kWh) net energy saved. An appropriately designed daylighting system can supply lighting at a cost of 2.5¢ to 5¢ per kWh [2].

### 7.1.3 Economic Basis for Passive Systems

The distinction between passive systems, active systems, and energy conservation is not critical for economic calculations. They are the same in all cases, a trade-off between the life cycle cost of the energy saved (performance) and the life cycle cost of the initial investment plus operating and maintenance costs (cost).

The key performance parameter to be determined is the net annual energy saved by the installation of the passive system. The basis for calculating the economics of any solar energy system is to compare it against a normal building. Thus, the actual difference in the annual cost of fuel is the difference in auxiliary energy that would be used with and without solar. The energy saved must be determined, rather than energy delivered, energy collected, useful energy, or some other energy measure. The other significant part of the economic trade-off involves determining the difference between the cost of construction of the passive building and that of the normal building against which it is to be compared, this is the "solar add-on cost." Again, this may be a difficult definition in the case of passive designs, because the building can be significantly altered compared to typical construction.

Passive solar water heaters are described in Chapter 5. This chapter describes passive space heating and cooling systems and daylighting.

## 7.2 PASSIVE SPACE-HEATING SYSTEMS

Passive heating systems contain the five basic components of all solar systems described in Chapters 4 and 5. Typically these are:

1. Collector—windows, walls and floors.
2. Storage—walls and floors, large interior masses (often integrated with the collector absorption function).
3. Distribution system—radiation, free convection, simple circulation fans.
4. Controls—moveable window insulation, vents both to other inside spaces or to ambient.
5. Backup system—any nonsolar heating system.



The design of passive heating systems requires the strategic placement of windows, storage masses, and the occupied spaces themselves. The fundamental principles of solar radiation geometry and availability are instrumental in the proper location and sizing of the system's collectors (windows). Storage devices are usually more massive than those used in active systems and are frequently an integral part of the collection and distribution system.

### 7.2.1 Types of Passive Heating Systems

A common method of cataloging the various passive system concepts distinguishes three general categories: direct, indirect, and isolated gain. Most of the physical configurations of passive heating systems are seen to fit within one or another of these three categories.

For direct gain systems (Figure 7.1), sunlight enters the heated space and is converted to heat at absorbing surfaces. This heat is then distributed throughout the space and to the various enclosing surfaces and room contents.

For indirect gain systems, sunlight is absorbed and stored by a mass interposed between the glazing and the conditioned space. The conditioned space is partially enclosed and bounded by this thermal storage mass, so a natural thermal coupling is achieved. Examples of the indirect approach are the thermal storage wall, the thermal storage roof, and the northerly room of an attached sunspace.

In the thermal storage wall (Figure 7.2a), sunlight penetrates the glazing and is absorbed and converted to heat at a wall surface interposed between the glazing and the heated space. The wall is usually masonry (Trombe wall) or containers filled with water (water wall), although it might contain phase-change material. The attached sunspace (Figure 7.2b) is actually a two-zone combination of direct gain and thermal storage wall. Sunlight enters and heats a direct gain southerly sunspace and a mass wall separating the northerly buffered space, which is heated indirectly. The sunspace is frequently used as a greenhouse, in which case the system is called an attached

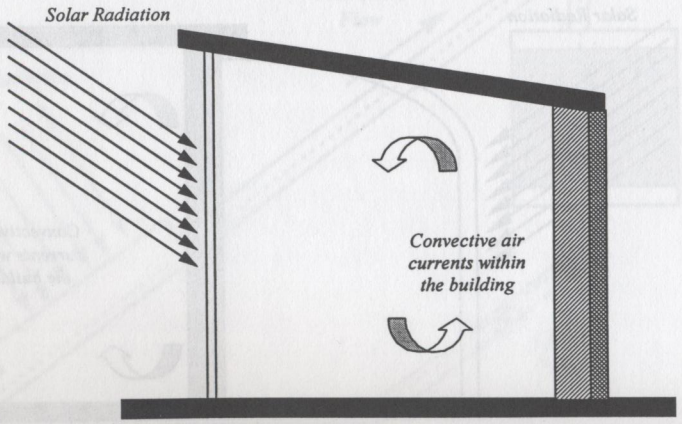


**Figure 7.1.** Concept of a direct gain passive heating system.

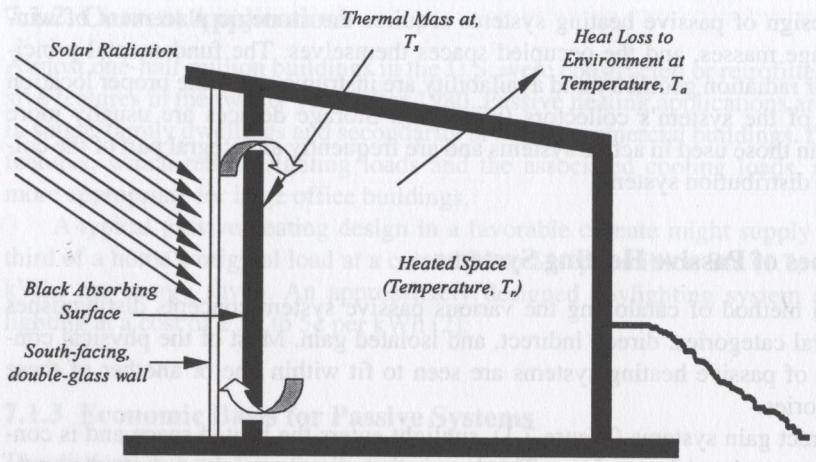


**Figure 7.2a.** Thermal Storage Wall.

greenhouse. The thermal storage roof (Figure 7.2c) is similar to the thermal storage wall except that the interposed thermal storage mass is located on the building roof. A thermal storage roof using water for storage and movable insulation on the top was developed by Hay [12] and is also known as the Roof-Pond system.

The isolated gain category concept is an indirect system, except that there is a distinct thermal separation (by means of either insulation or physical separation) between the thermal storage and the heated space. The convective (thermosyphon) loop, as depicted in Figure 7.3, is in this category and is often used to heat domestic water. It is most akin to conventional active systems in that there is a separate collector and separate thermal storage. It is a passive approach, however, because the thermal energy flow is by natural convection. The thermal storage wall, thermal storage roof, and attached sunspace approaches can also be made into isolated systems by insulating between the thermal storage and the heated space.

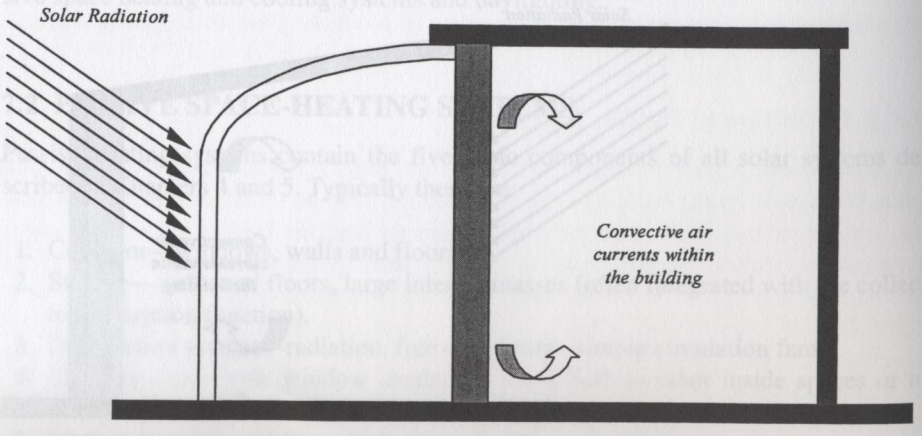


**Figure 7.2b.** Attached SunSpace.



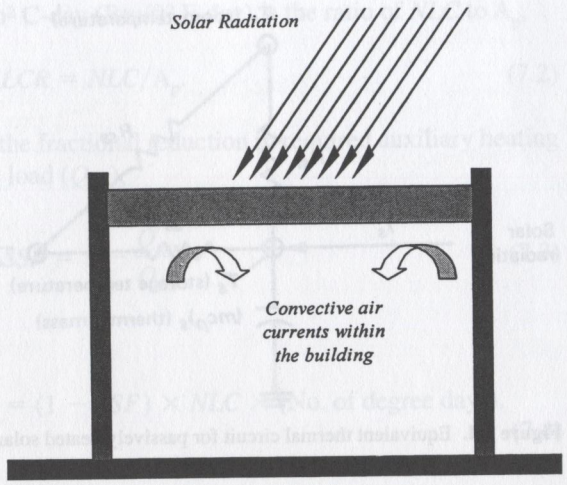


**Figure 7.2c.** Thermal Storage Roof.

## 7.2.2 Fundamental Concepts for Passive Heating Design

Figure 7.4 is an equivalent thermal circuit for the building illustrated in Figure 7.2a, the Trombe wall type system. For the heat transfer analysis of the building, three temperature nodes can be identified—room temperature, storage wall temperature, and ambient temperature. The circuit responds to climatic variables represented by a current injection $I_s$ (solar radiation) and by the ambient temperature $T_a$. The storage temperature $T_s$ and room temperature $T_r$ are determined by current flows in the equivalent circuit. By using seasonal and annual climatic data, the performance of a passive structure can be simulated, and the results of many such simulations correlated to give the design approaches described below.

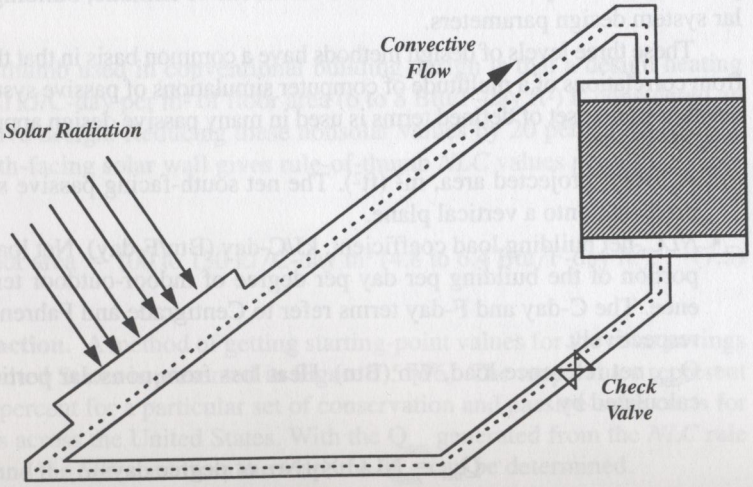


**Figure 7.3.** Convective Loop

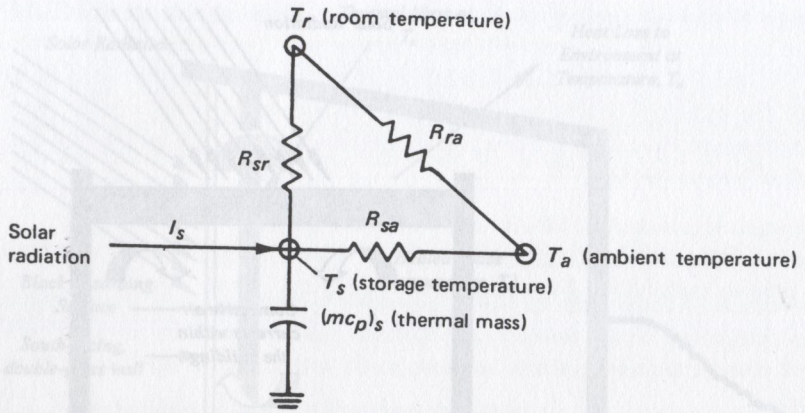


**Figure 7.4.** Equivalent thermal circuit for passively heated solar building in Fig. 7.2a.

### 7.2.3 Generalized Methods

Design of a passive heating system involves selection and sizing of the passive feature type(s), determination of thermal performance, and cost estimation. Ideally, a cost/performance optimization would be performed by the designer. Owner and architect ideas usually establish the passive feature type, with general size and cost estimation available. However, the thermal performance of a passive heating system has to be calculated.

There are several levels of methods that can be used to estimate the thermal performance of passive designs. First-level methods involve a rule of thumb and/or generalized calculation to get a starting estimate for size and/or annual performance. A second-level method involves climate, building, and passive system details. These details allow annual performance determination, plus some sensitivity to passive system design changes. Third-level methods involve periodic calculations (hourly, monthly) of performance and permit more detailed variations of climatic, building, and passive solar system design parameters.

These three levels of design methods have a common basis in that they all are derived from correlations of a multitude of computer simulations of passive systems [25,26]. As a result, a similar set of defined terms is used in many passive design approaches:

- $A_p$, solar projected area, m² (ft²). The net south-facing passive solar glazing area projected onto a vertical plane.
- *NLC*, net building load coefficient, kJ/C-day (Btu/F-day). Net load of the nonsolar portion of the building per day per degree of indoor-outdoor temperature difference. The C-day and F-day terms refer to Centigrade and Fahrenheit degree days, respectively.
- $Q_{net}$, net reference load, Wh (Btu). Heat loss from nonsolar portion of building as calculated by

$$Q_{net} = \text{NLC} \times (\text{No. of degree days}). \tag{7.1}$$



- *LCR*, load collector ratio, kJ/m² C-day (Btu/ft² F-day) is the ratio of *NLC* to $A_p$,

$$LCR = NLC/A_p. \tag{7.2}$$

- *SSF*, solar savings fraction, is the fractional reduction in required auxiliary heating ($Q_{aux}$) relative to net reference load ($Q_{net}$),

$$SSF = 1 - \frac{Q_{aux}}{Q_{net}}. \tag{7.3}$$

So, using Eq. (7.1),

$$\text{Auxiliary heat required, } Q_{aux} = (1 - SSF) \times NLC \times (\text{No. of degree days}). \tag{7.4}$$

The amount of auxiliary heat required is often a basis of comparison between possible solar designs. It is also the basis for determining building energy operating costs. Thus, many passive design methods are based on determining *SSF*, *NLC*, and the number of degree days in order to calculate the auxiliary heat required for a particular passive system by using Eq. (7.4).

### 7.2.4 The First Level: Rules of Thumb

A first estimate or starting value is needed to begin the passive system design process. Rules of thumb have been developed to generate initial values for solar aperture size, storage size, solar savings fraction, auxiliary heat required, and other size and performance characteristics. The following rules of thumb are meant to be used with the defined terms presented above.

**Load.** A rule of thumb used in conventional building design is that a design heating load of 120 to 160 kJ/C-day per m² of floor area (6 to 8 Btu/F-day ft²) is considered an energy conservative design. Reducing these nonsolar values by 20 percent to solarize the proposed south-facing solar wall gives rule-of-thumb *NLC* values per unit of floor area:

$$NLC/\text{Floor area} = 100 \text{ to } 130 \text{ kJ/C-day m}^2 \text{ (4.8 to 6.4 Btu/F-day ft}^2\text{)}. \tag{7.5}$$

**Solar savings fraction.** A method of getting starting-point values for the solar savings fraction in the United States is presented in Figure 7.5 [26]. The map values represent optimum *SSF* in percent for a particular set of conservation and passive-solar costs for different climates across the United States. With the $Q_{net}$ generated from the *NLC* rule of thumb above and the *SSF* read from the map, the $Q_{aux}$ can be determined.

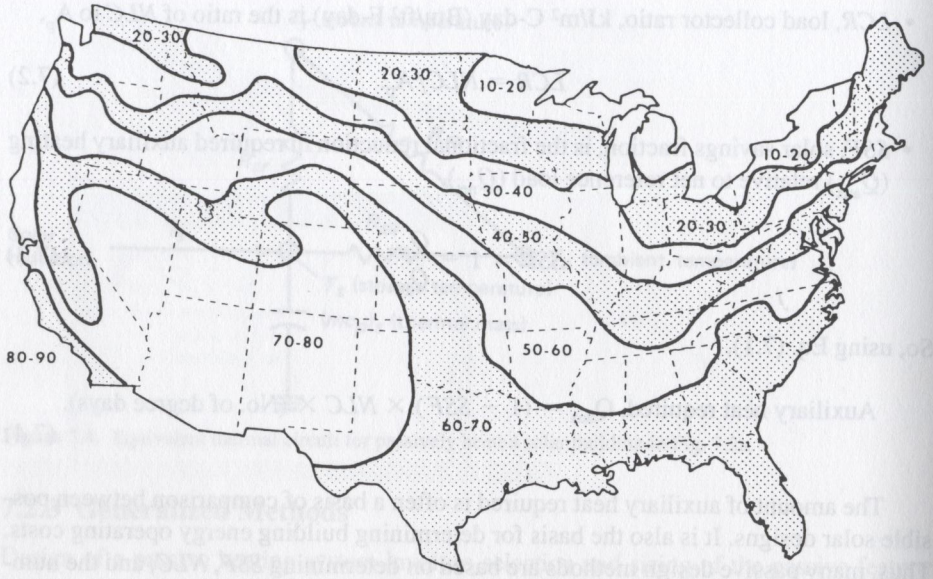


**Figure 7.5.** Starting-point values of solar savings fraction (SSF) in percent. *Source:* PSDH [26].

**LCR.** The $A_p$ can be determined using the *NLC* from above if the *LCR* is known. The rule of thumb associated with good values of *LCR* [27] differs depending on whether the design is for a cold or warm climate:

$$Good\ LCR = \begin{cases} \text{For cold climate: } 410\ \text{kJ/m}^2\ \text{C-day } (20\ \text{Btu/ft}^2\ \text{F-day}) \\ \text{For warm climate: } 610\ \text{kJ/m}^2\ \text{C-day } (30\ \text{Btu/ft}^2\ \text{F-day}) \end{cases} \quad (7.6)$$

**Storage.** Rules of thumb for thermal mass storage relate storage material total heat capacity to the solar projected area [26]. The use of the storage mass is to provide for heating on cloudy days and to regulate sunny day room air temperature swing. When the thermal mass direct absorbs the solar radiation, each square meter of the projected glazing area requires enough mass to store 613 kJ/C. If the storage material is not in direct sunlight, but heated from room air only, then four times as much mass is needed. In a room with a direct sunlight heated storage mass, the room air temperature swing will be approximately one-half the storage mass temperature swing. For room air heated storage, the air temperature swing is twice that of the storage mass.

A more location-dependent set of rules of thumb is presented in PSDH [25]. Comparing the results of that method to those of the method presented above, the two rules of thumb are seen to produce roughly similar answers. General system cost and performance information can be generated with results from rule-of-thumb calculations, but a more detailed level of information is needed to determine design-ready passive system type (direct gain, thermal wall, sunspace), size, performance, and costs.



### 7.2.5 The Second Level: *LCR* Method

The *LCR* method is useful for making estimates of the annual performance of specific types of passive system(s) combinations. The *LCR* method was developed by calculating the annual *SSF* for 94 reference passive solar systems for 219 U.S. and Canadian locations over a range of *LCR* values. Appendix Table A7.1 includes the description of these 94 reference systems for use both with the *LCR* method and with the *SLR* method described below. Tables were constructed for each city with *LCR* versus *SSF* listed for each of the 94 reference passive systems. (*Note:* The solar load ratio (*SLR*) method was used to make the *LCR* calculations. This *SLR* method is described in the next section as the third-level method.) While the complete *LCR* tables (PSDH, 1984) includes 219 locations, Appendix Table A7.2 includes only six representative cities (Albuquerque, Boston, Madison, Medford, Nashville, Santa Maria), due to space restrictions. The *LCR* method consists of the following steps [26]:

1. Determine the building parameters:
   a. Building load coefficient, *NLC*,
   b. Solar projected area, $A_p$, and
   c. Load collector ratio, $LCR = NLC/A_p$.
2. Find the short designation of the reference system closest to the passive system design (Table A7.1).
3. Enter the *LCR* Tables (Table A7.2):
   a. Find the city,
   b. Find the reference system designation,
   c. Determine annual *SSF* by interpolation using the *LCR* value from above, and
   d. Note the annual heating degree days (No. of degree days).
4. Calculate the annual auxiliary heat required:
   Auxiliary heat required = (1 - *SSF*) × *NLC* × (No. of degree days)

If more than one reference solar system is being used, then find the aperture area weighted *SSF* for the combination. Determine each individual reference system *SSF* using the total aperture area *LCR*, then take the area weighted average of the individual *SSF*s.

The *LCR* method allows no variation from the 94 reference passive designs. To treat off-reference designs, sensitivity curves have been produced that illustrate the effect on *SSF* of varying one or two design variables. These curves were produced for the six representative cities, which were chosen for their wide geographical and climatological ranges. Several of these sensitivity curves are presented in Appendix Figure A7.1.

Using the *LCR* method allows a basic design of passive system types for the 94 reference systems and the resulting annual performance. A bit more design variation can be obtained by using the sensitivity curves of Figure A7.1 to modify the *SSF* of a particular reference system. For instance, a storage wall system (Albuquerque, LCR = 72, thickness of 4 inches) *SSF* of 0.41 would increase by approximately 0.05, if the mass-area-to-glazing-area ratio (Am/Ag), assumed 6, were increased to 10, and would

decrease by about 0.06 if the mass-glazing-area ratio were decreased to 3. This information provides a designer with quantitative information for making trade-offs.

### 7.2.6 The Third Level: SLR Method

The solar-load ratio (SLR) method calculates monthly performance; the terms and values used are monthly based. The method allows the use of specific location weather data and the 94 reference design passive systems (Appendix Table A7.1). In addition, the sensitivity curves (Appendix Figure A7.1) can again be used to define performance outside the reference design systems. The result of the *SLR* method is the determination of the monthly heating auxiliary energy required, which is then summed to give the annual requirement for auxiliary heating energy. Generally, the *SLR* method gives annual values within ±3% of detailed simulation results, but the monthly values may vary more [7,26]. Thus, the monthly *SLR* method is more accurate than the rule-of-thumb methods, and it provides the designer with system performance on a month-by-month basis.

The *SLR* method uses equations and correlation parameters for each of the 94 reference systems in combination with the insolation absorbed by the system, the monthly degree days, and the system's *LCR* to determine the monthly *SSF*. These correlation parameters are listed in Appendix Table A7.3 as *A, B, C, D, R, G, H,* and *LCR*s for each reference system [26]. The correlation equations are

$$SSF = 1 - K(1 - F), \tag{7.7}$$

where

$$K = 1 + G/LCR, \tag{7.8}$$

$$F = \begin{cases} AX, \text{ when } X < R \\ B - C\exp(-DX), \text{ when } X > R \end{cases} \tag{7.9}$$

$$X = \frac{S/DD - (LCRs)H}{(LCR)K}, \tag{7.10}$$

and $X$ is called the generalized solar load ratio. The *DD* term is the monthly number of degree-days. The term $S$ is the monthly insolation absorbed by the system per unit of solar projected area. Monthly average daily insolation data on a vertical south facing surface can be found or calculated using various sources [21,26]. The $S$ term can be determined by multiplying by a transmission and an absorption factor and the number of days in the month. Absorption factors for all systems are close to 0.96 [21], whereas the transmission is approximately 0.9 for single glazing, 0.8 for double glazing, and 0.7 for triple glazing.

**Example 7.1.** For a vented, 180 ft², double-glazed with night insulation, 12″ thick Trombe wall system (TWD4) in a *NLC* = 11,800 Btu/F-day house in Medford, Oregon, determine the auxiliary energy required in January.



**Solution.** Weather data for Medford, Oregon [26], yields for January ($N$ = 31 days): daily vertical surface insolation = 565 Btu/ft² and *DD* = 880 F-days; so $S$ = (31)(565)(0.8)(0.96) = 13,452 Btu/ft² -month.

$$LCR = NLC/A_p = 11{,}800/180 = 65.6 \text{ Btu/F-day ft}^2.$$

From Table A7.3 at TWD4: $A = 0$, $B = 1$, $C = 1.0606$, $D = 0.977$, $R = -9$, $G = 0$, $H = 0.85$, *LCR*s = 5.8 Btu/F-day ft².

Substituting into Eq. (7.8) gives

$$K = 1 + 0/65.6 = 1.$$

Eq. (7.10) gives

$$X = \frac{13{,}452/880 - (5.8 \times 0.85)}{65.6 \times 1} = 0.16.$$

Eq. (7.9) gives

$$F = 1 - 1.0606\, e^{-0.977 \times 0.16} = 0.09,$$

and Eq. (7.7) gives

$$SSF = 1 - 1(1 - 0.09) = 0.09.$$

The January auxiliary energy required can be calculated using Eq. (7.4):

$$\begin{aligned} Q_{aux}(\text{Jan}) &= (1 - SSF) \times NLC \times (\text{No. of degree days}) \\ &= (1 - 0.09) \times 11{,}800 \times 880 \\ &= 9{,}450{,}000 \text{ Btu}. \end{aligned}$$

As mentioned, the use of sensitivity curves [26] as in Figure A7.1 will allow *SSF* to be determined for many off-reference system design conditions involving storage mass, number of glazings, and other more esoteric parameters. Also, the use of multiple passive system types within one building would be approached by calculating the *SSF* for each type system individually using a combined area *LCR*, and then a weighted-area (aperture) average *SSF* would be determined for the building.

## 7.3 PASSIVE SPACE-COOLING SYSTEMS

Passive cooling systems are designed to use natural means to transfer heat from buildings by means of convection/ventilation, evaporation, radiation, and conduction. However, the most important element in both passive and conventional cooling design is to

prevent heat from entering the building in the first place. Cooling conservation techniques involve building surface colors, insulation, special window glazings, overhangs and orientation, and numerous other architectural and engineering features.

### 7.3.1 Controlling the Solar Input

Controlling the solar energy input to reduce the cooling load is usually considered a passive (versus a conservation) design concern because solar input may be needed for other purposes, such as daylighting throughout the year or heating during the winter or both. Basic architectural solar control is normally designed in via the shading of the solar windows, where direct radiation is desired for winter heating and needs to be excluded during the cooling season.

The shading control of the windows can be of various types and controlability, ranging from drapes and blinds, to use of deciduous trees, to commonly used overhangs and vertical louvers. A rule-of-thumb design for determining proper south-facing window overhang for both winter heating and summer shading is presented in Table 7.1. Technical details on calculating shading from various devices and orientations are found in ASHRAE [3] and Olgyay and Olgyay [23].

**Table 7.1. South-facing window overhang rule of thumb**

$$\text{Length of the Overhang} = \frac{\text{Window Height}}{F}$$

(a) Overhang Factors

| North Latitude | F* |
|---|---|
| 28 | 5.6–11.1 |
| 32 | 4.0–6.3 |
| 36 | 3.0–4.5 |
| 40 | 2.5–3.4 |
| 44 | 2.0–2.7 |
| 48 | 1.7–2.2 |
| 52 | 1.5–1.8 |
| 56 | 1.3–1.5 |

(b) Roof Overhang Geometry

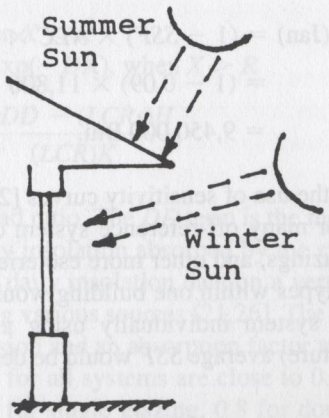


Properly sized overhangs shade out hot summer sun but allow winter sun (which is lower in the sky) to penetrate windows.

*Select a factor according to your latitude. Higher values provide complete shading at noon on June 21; lower values, until August 1.

*Source:* Halacy [11].



### 7.3.2 Movement of Air

Air movement provides cooling comfort through convection and evaporation from human skin. ASHRAE [3] places the comfort limit at 79°F (26°C) for an air velocity of 50 ft/min (0.25 m/s) (fpm), 82°F for 160 fpm, and 85°F for 200 fpm. To determine whether or not comfort conditions can be obtained, a designer must calculate the volumetric flow rate, $Q$, which is passing through the occupied space. Using the cross-sectional area, $A_x$, of the space and the room air velocity, $V_a$, required, the flow is determined by

$$Q = A_x V_a. \tag{7.11}$$

The proper placement of windows, narrow building shape, and open landscaping can enhance natural wind flow to provide ventilation. The air flow rate through open windows for wind-driven ventilation is given by ASHRAE [3]:

$$Q = C_v V_w A_w, \tag{7.12}$$

where $Q$ = air flow rate, m³/s
$A_w$ = free area of inlet opening, m²
$V_w$ = wind velocity, m/s
$C_v$ = effectiveness of opening = 0.5 to 0.6 for wind perpendicular to opening, and 0.25 to 0.35 for wind diagonal to opening

The stack effect can induce ventilation when warm air rises to the top of a structure and exhausts outside, while cooler outside air enters the structure to replace it. Figure 7.6 illustrates the solar chimney concept, which can easily be adapted to a thermal storage wall system. The greatest stack-effect flow rate is produced by maximizing the stack height and the air temperature in the stack, as given by

$$Q = 0.116 A_j \sqrt{h(T_s - T_o)}, \tag{7.13}$$

where $Q$ = stack flow rate, m³/s,
$A_j$ = area of inlets or outlets (whichever is smaller), m²,
$h$ = inlet to outlet height, m,
$T_s$ = average temperature in stack, °C, and
$T_o$ = outdoor air temperature, °C.

If either the inlet or outlet area is twice the other, the flow rate will increase by 25 percent, and if the area ratio is 3:1 or larger, it will increase by 35 percent.

**Example 7.2.** A two-story (5 m) solar chimney is being designed to produce a flow of 0.25 m³/s through a space. The preliminary design features include a 25 cm × 1.5 m inlet, a 50 cm × 1.5 m outlet, and an estimated 35°C average stack temperature on a sunny 30°C day. Can this design produce the desired flow?

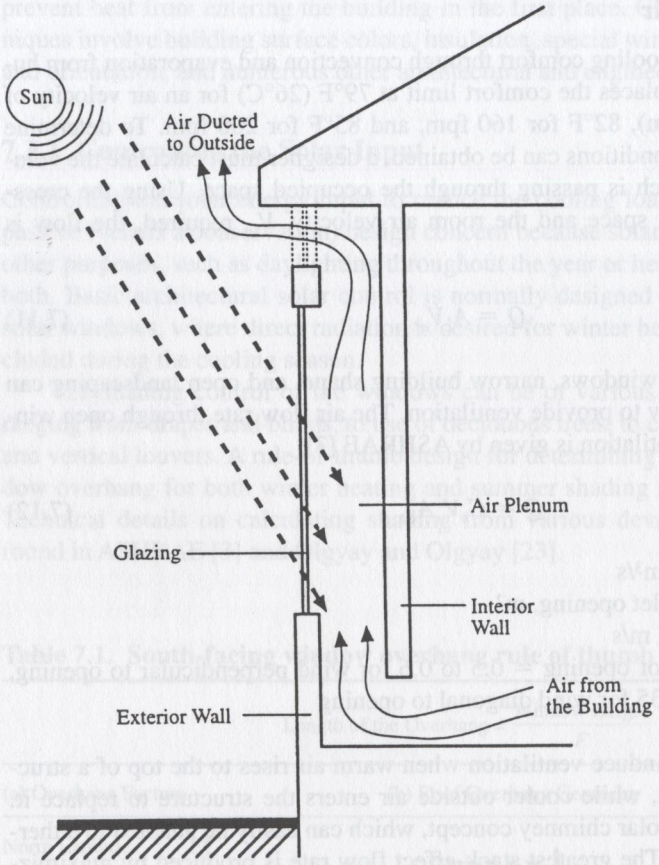


**Figure 7.6.** The stack-effect/solar chimney concept to induce convection/ventilation. *Source:* PSDH [25].

**Solution.** Substituting the design data into Eq. (7.13):

$$Q = 0.116(.25 \times 1.5)[5(5)]^{1/2}$$
$$= 0.2 \text{ m}^3/\text{s}.$$

Since the outlet area is twice the inlet area, the 25 percent flow increase can be used:

$Q = 0.2\ (1.25) = 0.25\ \text{m}^3/\text{s}$ (Answer: Yes, the proper flow rate is obtained.)

### 7.3.3 Evaporative Cooling

When air with less than 100 percent relative humidity moves over a water surface, the evaporation of water causes both the air and the water itself to cool. The lowest temperature that can be reached by this direct evaporative cooling effect is the wet-bulb temperature of the air, which is directly related to the relative humidity, lower wet-bulb temperature being associated with lower relative humidity. Thus, dry air (low relative humidity) has a low wet-bulb temperature and will undergo a large temperature drop with evaporative cooling, while humid air (high relative humidity) can only be slightly cooled evaporatively. The wet-bulb temperature for various relative humidity and air temperature conditions can be found via the psychrometric chart available in most thermodynamic texts. Normally, an evaporative cooling process cools the air only part of the way down to the wet-bulb temperature. To get the maximum temperature decrease, it is necessary to have a large water surface area in contact with the air for a long time. Interior ponds and fountain sprays are often used to provide this air-water contact area.

The use of water sprays and open ponds on roofs provides cooling primarily via evaporation. The hybrid system involving a fan and wetted mat, the swamp cooler, is by far the most widely used evaporative cooling combined design. Features are described in ASHRAE [3,4].



### 7.3.4 Nocturnal Cooling Systems

Another approach to passive convective/ventilative cooling involves using cooler night air to reduce the temperature of the building or of a storage mass. Thus, the building/storage mass is prepared to accept part of the heat load during the hotter daytime. This type of convective system can also be combined with evaporative and radiative modes of heat transfer, utilizing air or water, or both, as the convective fluid. Work in Australia [5] investigated rock storage beds that were chilled using evaporatively cooled night air. Room air was then circulated through the bed during the day to provide space cooling. The use of encapsulated roof ponds as a thermal cooling mass has been tried by several investigators [12,19] and is often linked with nighttime radiative cooling.

All warm objects emit thermal infrared radiation; the hotter the body, the more energy it emits. A passive cooling scheme uses the cooler night sky as a sink for thermal radiation emitted by a warm storage mass, thus chilling the mass for cooling use the next day. The net radiative cooling rate, $Q_r$, for a horizontal unit surface [3] is

$$Q_r = \epsilon\sigma\,(T_{\text{body}}^4 - T_{\text{sky}}^4), \tag{7.14}$$

where $Q_r$ = net radiative cooling rate, W/m² (Btu/h ft²),
$\epsilon$ = surface emissivity (usually 0.9 for water),
$\sigma = 5.67 \times 10^{-8}$ W/m² K⁴ ($1.714 \times 10^{-9}$ Btu/h ft² R⁴),
$T_{\text{body}}$ = warm body temperature, Kelvin (Rankine), and
$T_{\text{sky}}$ = effective sky temperature, Kelvin (Rankine).

The monthly average air-sky temperature difference has been determined [20] and Figure 7.7 presents these values for July (in °F) for the United States.

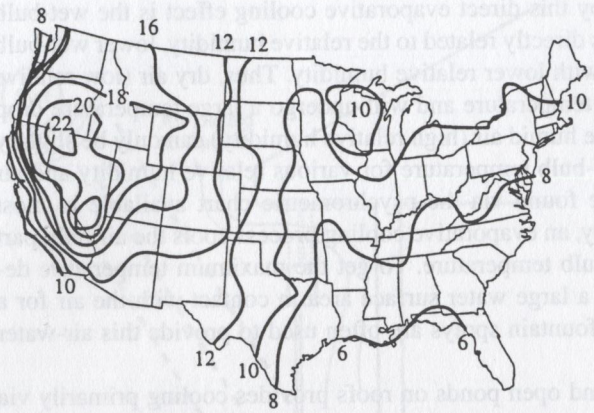


**Figure 7.7.** Average monthly sky temperature depression ($T_{air} - T_{sky}$) for July in °F. Adapted from Martin and Berdahl [20].

**Example 7.3.** Estimate the overnight cooling possible for a 10 m², 85°F water thermal storage roof during July in Los Angeles.

**Solution.** Assume the roof storage unit is black with $\epsilon = 0.9$. From Figure 7.7, $T_{air} - T_{sky}$ is approximately 10°F for Los Angeles. From weather data for LA airport, [3,27], the July average temperature is 69°F with a range of 15°F. Assuming night temperatures vary from the average (69°F) down to half the daily range (15 × 1/2), then the average nighttime temperature is chosen as 69 − (1/2)(15/2) = 65°F. So, $T_{sky}$ = 65 − 10 = 55°F. From Eq. (7.14),

$$Q_r = 0.9\,(1.714 \times 10^{-9})[(460 + 85)^4 - (460 + 55)^4]$$
$$= 27.6 \text{ Btu/h ft}^2$$

For a 10-hour night and 10 m² (107.6 ft²) roof area,

$$\text{Total radiative cooling} = 27.6\,(10)(107.6)$$
$$= 29{,}700 \text{ Btu}$$

*Note:* This does not include the convective cooling possible which can be approximated (at its maximum rate) for still air [3] by

$$\text{Maximum total } Q_{conv} = hA(T_{roof} - T_{air})(\text{Time})$$
$$= 5(129)(85 - 55)(10)$$
$$= 161{,}000 \text{ Btu}$$



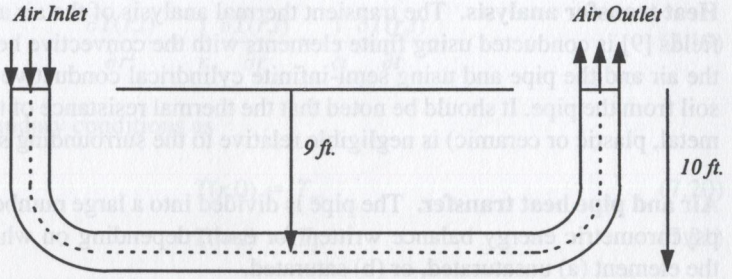


**Figure 7.8a.** Open loop underground air tunnel system.

This is a maximum since the 85°F storage temperature will drop as it cools, which is also the case for the radiative cooling calculation. However, convection is seen to usually be the more dominant mode of nighttime cooling.

### 7.3.5 Earth Contact Cooling (or Heating)

Earth contact cooling or heating is a passive summer cooling and winter heating technique that utilizes underground soil as the heat sink or source. By installing a pipe underground and passing air through the pipe, the air will be cooled or warmed depending on the season. Schematics of an open loop system and a closed loop air-conditioning system are presented in Figures 7.8a and 7.8b, respectively [8].

The use of this technique can be traced back to 3000 B.C. when Iranian architects designed some buildings to be cooled by natural resources only. In the 19th century, Wilkinson [29] designed a barn for 148 cows where a 500-ft long underground passage was used for cooling during the summertime. Since that time, a number of experimental and analytical studies of this technique have appeared in the literature. Goswami and Dhaliwal [9] have given a brief review of the literature and presented an analytical solution to the problem of transient heat transfer between the air and the surrounding soil as the air is made to pass through a pipe buried underground. More recently, Krarti and Kreider [14] have also presented an analytical model for heat transfer in an underground air tunnel.

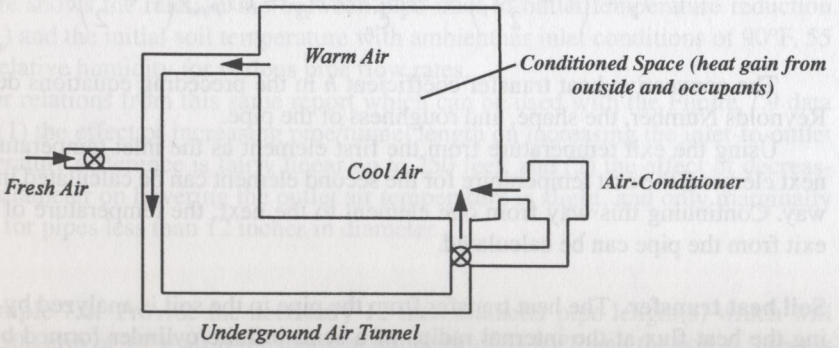


**Figure 7.8b.** Schematic of closed loop air-conditioning system using air-tunnel.

**Heat transfer analysis.** The transient thermal analysis of the air and soil temperature fields [9] is conducted using finite elements with the convective heat transfer between the air and the pipe and using semi-infinite cylindrical conductive heat transfer to the soil from the pipe. It should be noted that the thermal resistance of the pipe (whether of metal, plastic or ceramic) is negligible relative to the surrounding soil.

**Air and pipe heat transfer.** The pipe is divided into a large number of elements and a psychrometric energy balance written for each, depending on whether the air leaves the element (a) unsaturated, or (b) saturated.

(*a*) If the air leaves an element as unsaturated, the energy balance on the element is:

$$mc_p(T_1 - T_2) = hA_p(T_{air} - T_{pipe}), \tag{7.15}$$

$T_{air}$ can be taken as $\dfrac{T_1 + T_2}{2}$.

Substituting and simplifying we get

$$T_2 = \left[\left(1 - \frac{U}{2}\right)T_1 + UT_{pipe}\right] \Big/ \left(1 + \frac{U}{2}\right), \tag{7.16}$$

where $U$ is defined as

$$U = \frac{A_p h}{mc_p}.$$

(b) If the air leaving the element is saturated, the energy balance is

$$mC_pT_1 + m(W_1 - W_2)H_{fg} = mC_pT_2 + hA_p(T_{air} - T_{pipe}). \tag{7.17}$$

Simplifying we get:

$$T_2 = \left(1 - \frac{U}{2}T_1\right) + \frac{W_1 - W_2}{C_p}H_{fg} + UT_{Pipe} \Big/ \left(1 + \frac{U}{2}\right). \tag{7.18}$$

The convective heat transfer coefficient $h$ in the preceding equations depends on Reynolds Number, the shape, and roughness of the pipe.

Using the exit temperature from the first element as the inlet temperature for the next element, the exit temperature for the second element can be calculated in a similar way. Continuing this way from one element to the next, the temperature of air at the exit from the pipe can be calculated.

**Soil heat transfer.** The heat transfer from the pipe to the soil is analyzed by considering the heat flux at the internal radius of a semi-infinite cylinder formed by the soil around the pipe. For a small element the problem can be formulated as



$$\frac{\partial T(r,t)}{\partial r^2} + \frac{1}{r}\frac{\partial T(r,t)}{\partial r} = \frac{1}{\alpha}\frac{\partial T(r,t)}{\partial t}, \tag{7.19}$$

with initial and boundary conditions as

$$T(r,0) = T_e, \tag{7.20}$$

$$T(\infty,t) = T_e, \tag{7.21}$$

$$-K\frac{\partial T}{\partial r}(r,t) = q'', \tag{7.22}$$

where $T_e$ is the bulk earth temperature and $q''$ is also given by the amount of heat transferred to the pipe from the air by convection, i.e., $q'' = h(T_{air} - T_{pipe})$.

**Soil temperatures and properties.** Labs [17] studied the earth temperatures in the United States. According to this study, temperature swings in the soil during the year are dampened with depth below the ground. There is also a phase lag between the soil temperature and the ambient air temperature. This phase lag increases with depth below the surface. For example, the soil temperature for light dry soil at a depth of about 10 ft (3.05m) varies by approximately ± 5°F (2.8°C) from the mean temperature (approximately equal to mean annual air temperature) and has a phase lag of approximately 75 days behind ambient air temperature [17].

The thermal properties of the soil are difficult to determine. The thermal conductivity and diffusivity both change with the moisture content of the soil itself, which is directly affected by the temperature of and heat flux from and to the buried pipe. Most researchers have found that using constant property values for soil taken from standard references gives reasonable predictive results [10].

**Generalized results from experiments.** Figure 7.9 presents data from Goswami and Biseli [8] for an open system, 100-foot long, 12-inch diameter pipe, buried 9 feet deep. The figure shows the relationship between pipe inlet-to-outlet temperature reduction ($T_{in} - T_{out}$) and the initial soil temperature with ambient air inlet conditions of 90°F, 55 percent relative humidity for various pipe flow rates.

Other relations from this same report which can be used with the Figure 7.9 data include: (1) the effect of increasing pipe/tunnel length on increasing the inlet-to-outlet air temperature difference is fairly linear up to 250 feet; and (2) the effect of decreasing pipe diameter on lowering the outlet air temperature is slight, and only marginally effective for pipes less than 12 inches in diameter.

**Example 7.4.** Provide the necessary 12-inch diameter pipe length(s) which will deliver 1500 cfm of 75°F air if the ambient temperature is 85°F and the soil at 9 feet is 65°F.

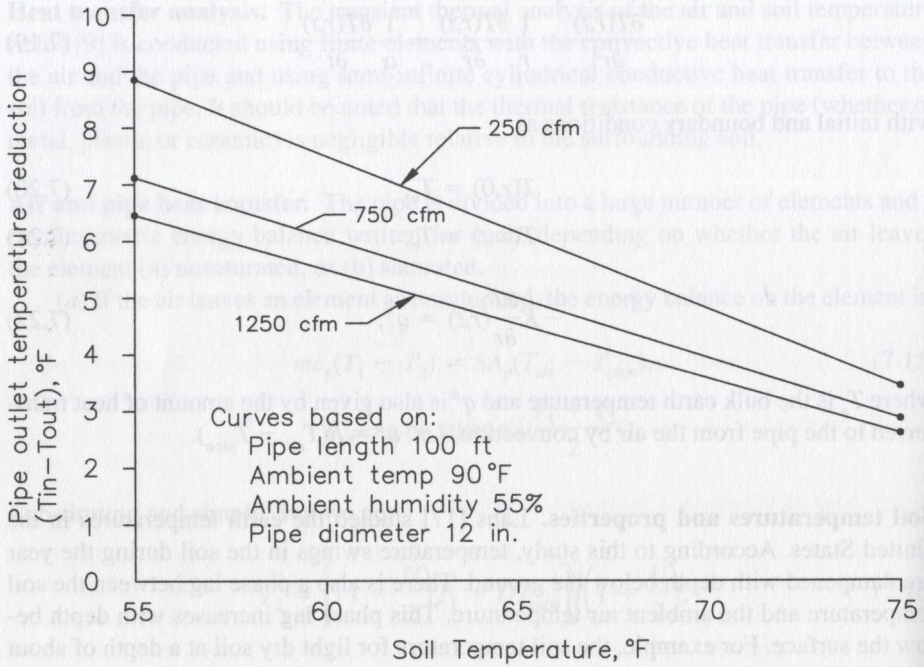


**Figure 7.9.** Air temperature drop through a 100-ft long, 12-inch diameter pipe buried 9 feet underground.

**Solution.** From Fig. 7.9, for 100 ft. of pipe at 70°F soil temperature (use 70°F to keep the same ambient-to-soil temperature as is used in Fig. 7.9), the pipe temperature reduction is

$$T_{in} - T_{out} = 5°F \text{ (at 250 cfm)},$$
$$= 4°F \text{ (at 750 cfm), and}$$
$$= 3.5°F \text{ (at 1250 cfm).}$$

Since the length versus temperature reduction is linear (see text above), the 10°F reduction required (85°F down to 75°F) would be met by the 750 cfm case (4°F for 100 ft) if 250 ft of pipe is used. Then, two 12-inch diameter pipes would be required to meet the 1500 cfm requirement.

Answer: Two 12-inch diameter pipes, each 250 ft long. (Note: See what would be needed if the 250 cfm or the 1250 cfm cases had been chosen. Which of the three flow rate cases leads to the least expensive installation?)

## 7.4 DAYLIGHTING FUNDAMENTALS

Daylighting is the use of the sun's radiant energy to illuminate the interior spaces in a building. In the last century, electric lighting was considered an alternative technology



to daylighting. Today the situation is reversed, primarily due to the economics of energy use and conservation. However, there are good physiological reasons for using daylight as an illuminant. The quality of daylight matches the human eye's response, thus permitting lower light levels for task comfort, better color rendering, and clearer object discrimination [27].

**Lighting terms and units.** Measurement of lighting level is based on the standard candle, where the lumen (lm), the unit of luminous flux ($\Phi$), is defined as the rate of luminous energy passing through a 1 square meter area located 1 meter from the candle. Thus, a standard candle generates $4\pi$ lumens which radiate away in all directions. The illuminance ($E$) on a surface is defined as the luminous flux on the surface divided by the surface area, $E = \Phi/A$. Illuminance is measured in either lux (lx), as lumens per square meter, or footcandles (fc), as lumens per square foot.

Determination of the daylighting available in a building space at a given location and time is important in order to evaluate the reduction possible in electric lighting and to determine the associated impact on heating and cooling loads. Daylight provides about 110 lm/W of solar radiation, fluorescent lamps about 75 lm/W of electrical input, and incandescent lamps about 20 lm/W; thus daylighting generates only 1/2 to 1/5 the heating that equivalent electric lighting does, significantly reducing the building cooling load.

### 7.4.1 Economics of Daylighting

The economic benefit of daylighting is directly tied to the reduction in lighting electrical energy operating costs. Also, lower cooling system operating costs are possible due to the reduction in heating caused by the reduced electrical lighting load. The reduction in lighting and cooling system electrical power during peak demand periods could also beneficially affect demand charges.

The reduction of the design cooling load through the use of daylighting can also lead to the reduction of installed or first-cost cooling system dollars. Normally, economics dictate that an automatic lighting control system must take advantage of the reduced lighting/cooling effect, and the control system cost, minus any cooling system cost, savings should be expressed as a net first cost. A payback time for the lighting control system (net or not) can be calculated from the ratio of first costs to yearly operating savings. In some cases, these paybacks for daylighting controls have been found to be in the range of 1 to 5 years for office building spaces [28].

Controls, both aperture and lighting, directly affect the efficacy of the daylighting system. As shown in Figure 7.10, aperture controls can be architectural (overhangs, light shelves, etc.) or window shading devices (blinds, automated louvers, etc.). The aperture controls generally moderate the sunlight entering the space to maximize or minimize solar thermal gain, permit the proper amount of light for visibility, and prevent glare and beam radiation onto the workplace. Photosensor control of electric lighting allows the dimming (or shutting off) of the lights in proportion to the amount of available daylighting illuminance.

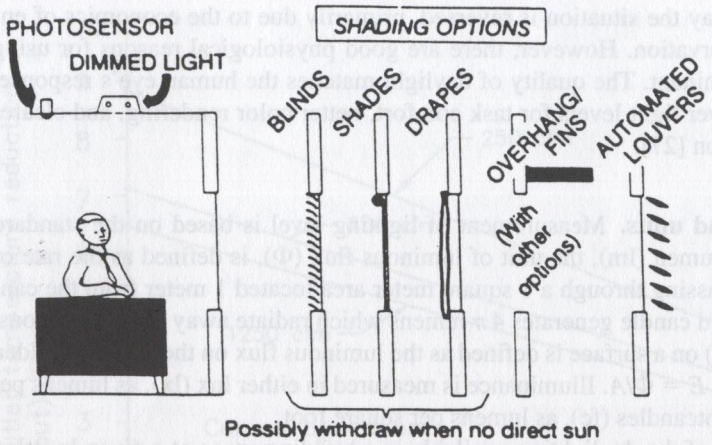


**Figure 7.10.** Daylighting system controls. *Source:* Rundquist [29].

In most cases, using daylighting controls to increase the solar gain for daylighting purposes saves more in electrical lighting energy and in cooling energy associated with the lighting than is incurred with the added solar gain [28]. In determining the annual energy savings from daylighting ($ES_T$), the annual lighting energy saved from daylighting ($ES_L$) is added with the reduction in cooling system energy ($\nabla ES_C$) and with the negative of the heating system energy increase ($\nabla ES_H$):

$$ES_T = ES_L + \nabla ES_C - \nabla ES_H. \tag{7.23}$$

A simple approach to estimating the heating and cooling energy changes associated with lighting energy reduction is to use the fraction of the year associated with the cooling or heating season ($f_c$,$f_H$) and the seasonal *COP* of the cooling or heating equipment. Thus, Eq. (7.23) can be expressed as

$$ES_T = ES_L + \frac{f_c ES_L}{COP_c} - \frac{f_H ES_L}{COP_H},$$

$$= ES_L\left(1 + \frac{f_c}{COP_c} - \frac{f_H}{COP_H}\right). \tag{7.24}$$

It should be noted that the increased solar gain due to daylighting has not been included here but would reduce summer savings and increase winter savings. If it is assumed that the increased wintertime daylighting solar gain approximately offsets the reduced lighting heat gain, then the last term in Eq. (7.24) becomes negligible.



### 7.4.2 Daylighting Design Fundamentals

As mentioned, aperture controls such as blinds and drapes are used to moderate the amount of daylight entering the space, as are the architectural features of the building itself (glazing type, area, orientation; overhangs and wingwalls, lightshelves, etc.). Dimming controls are used to adjust the electric light level based on the quantity of the daylighting. With these two types of controls (aperture and lighting), the electric lighting and cooling energy use and demand, as well as cooling system size, can be reduced. However, the determination of the daylighting position and time **illuminance** value within the space is required before energy usage and demand reduction calculations can be made.

**Architectural features.** Daylighting design approaches use both solar beam radiation (sunlight) and the diffuse radiation scattered by the atmosphere (skylight) as sources for interior lighting, with historical design emphasis being on utilizing skylight. Daylighting is provided through a variety of glazing features which can be grouped as sidelighting (light entering via the side of the space) and toplighting (light entering from the ceiling area). Figure 7.11 illustrates several architectural forms producing sidelighting and toplighting. The dashed lines represent the illuminance distribution within the space. Calculation of workplane illuminance depends on whether sidelighting or toplighting features are used. The combined illuminance values are additive.

**Daylighting geometry.** The solar illuminance on a vertical or horizontal window depends on the position of the sun relative to that window. In the method described here, the sun and sky illuminance values are determined using the sun's altitude angle ($\alpha$) and the sun-window azimuth angle difference ($a_{sw}$). These angles need to be determined for the particular time of day, day of year, and window placement under investigation.

***Solar altitude angle ($\alpha$).*** The solar altitude angle is the angle swept out by a person's arm when pointing to the horizon directly below the sun and then raising the arm to point at the sun. Equation (2.28) can be used to calculate solar altitude, $\alpha$, as

$$\sin\alpha = \cos L \cos\delta_s \cos h_s + \sin L \sin\delta_s. \tag{2.28}$$

***Sun-window azimuth angle difference ($a_{sw}$).*** The difference between the sun's azimuth and the window's azimuth needs to be calculated for vertical window illuminance. The window's azimuth angle, $a_w$, is determined by which way it faces, as measured from south (east of south is negative, westward is positive). The solar azimuth angle, $a_s$, is calculated using Eq. (2.29):

$$\sin a_s = \cos\delta_s \sin h_s/\cos\alpha. \tag{2.29}$$

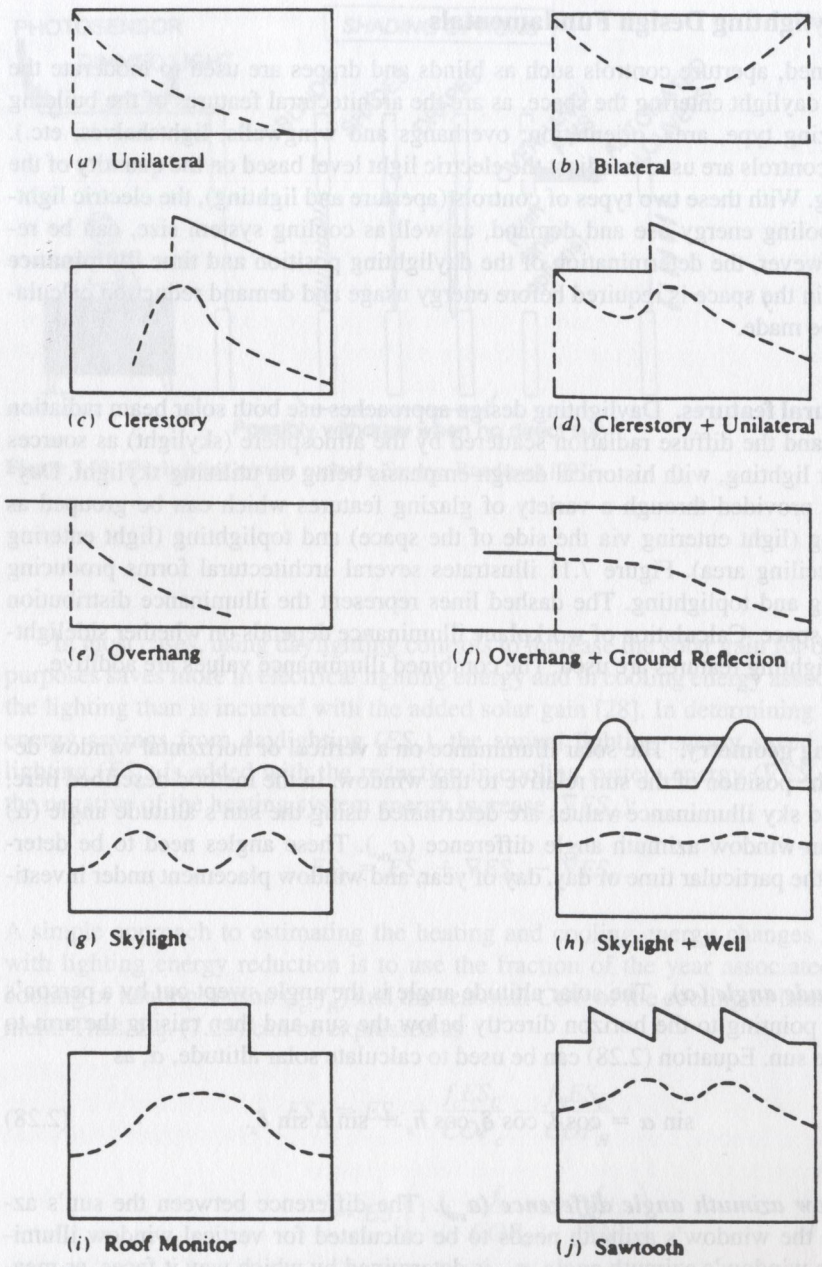


**Figure 7.11.** Example of sidelighting and toplighting architectural features. (Dashed lines represent illuminance distributions.) *Source:* Murdoch [22].



The sun-window azimuth angle difference, $a_{sw}$, is given by the absolute value of the difference between $a_s$ and $a_w$:

$$a_{sw} = |a_s - a_w|. \tag{7.25}$$

### 7.4.3 Design Methods

To determine the annual lighting energy saved ($ES_L$) for the space under investigation, calculations using the lumen method described below should be performed on a monthly basis for both clear and overcast days. Monthly weather data for the site would then be used to prorate clear and overcast lighting energy demands each month. Subtracting the calculated daylighting illuminance from the design illuminance leaves the supplementary lighting needed, which determines the lighting energy required.

The approach in the method below is to calculate the sidelighting and the skylighting of the space separately and then combine the results. This procedure has been computerized and includes many details of controls, daylighting methods, weather, and heating and cooling load calculations. ASHRAE [3] lists many of the methods and simulation techniques currently used with daylighting and its associated energy effects.

### 7.4.4 Lumen Method of Sidelighting (Vertical Windows)

The lumen method of sidelighting calculates interior horizontal illuminance at three points, as shown in Figure 7.12, along the 30-inch (0.76 m) work plane on the room-and-window centerline. A vertical window is assumed to extend from 36 inches (0.91 m) above the floor to the ceiling. The method accounts for both direct and ground-

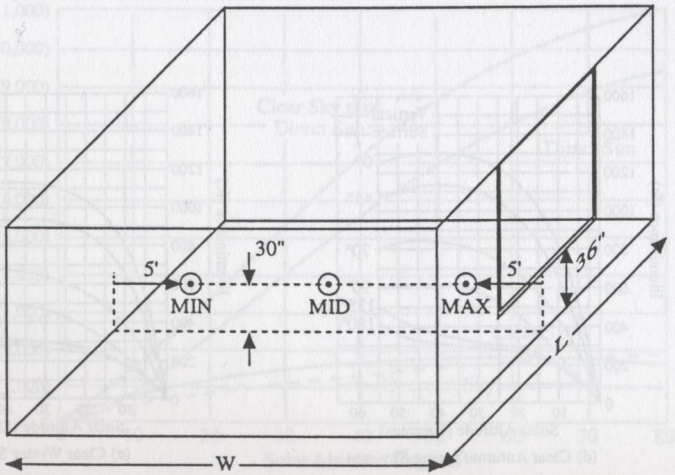


**Figure 7.12.** Location of illumination points within the room (along centerline of window) determined by lumen method of sidelighting.

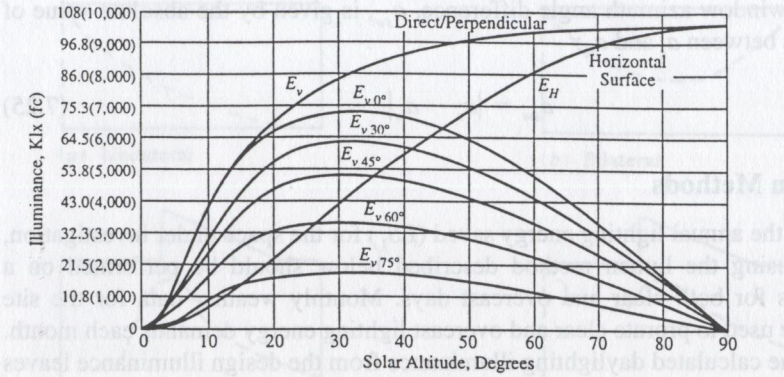


(a) Direct Sunlight

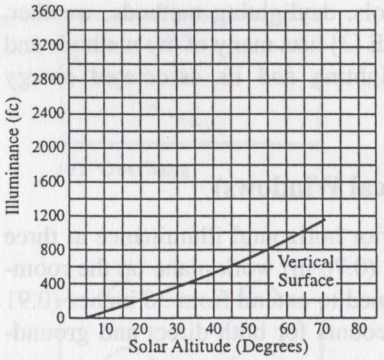


(b) Overcast Skylight

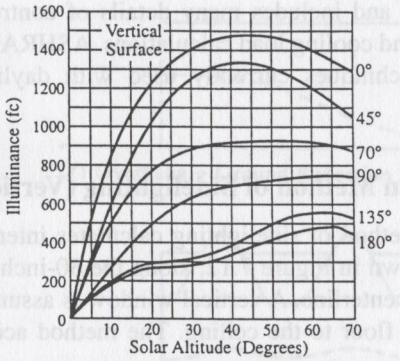


(c) Clear Summer Skylight

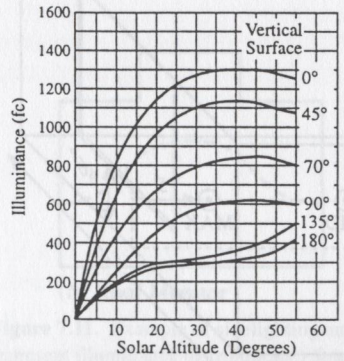


(d) Clear Autumn/Spring Skylight

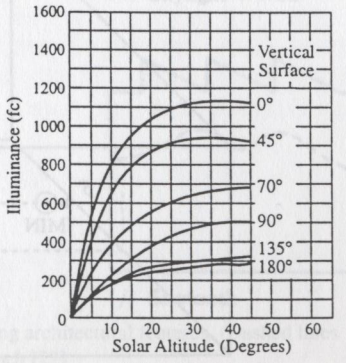


(e) Clear Winter Skylight

**Figure 7.13.** Vertical illuminance from (a) direct sunlight and (b–e) skylight, for various sun-window azimuth angle differences. *Source:* IES [13].



reflected sunlight and skylight, so both horizontal and vertical illuminances from sun and sky are needed. The steps in the lumen method of sidelighting are presented next.

The incident direct and ground-reflected window illuminance are normally calculated for both a cloudy and a clear day for representative days during the year (various months), as well as for clear or cloudy times during a given day. Thus, the interior illumination due to sidelighting and skylighting can then be examined for effectiveness throughout the year.

**Step 1: Incident direct sky and sun illuminances.** The solar altitude and sun-window azimuth angle difference are calculated for the desired latitude, date, and time using Eqs. (2.28) and (7.25), respectively. Using these two angles, the total illuminance on the window ($E_{sw}$) can be determined by summing the direct sun illuminance ($E_{uw}$) and the direct sky illuminance ($E_{kw}$), each determined from the appropriate graph in Figure 7.13.

**Step 2: Incident ground-reflected illuminance.** The sun illuminance on the ground ($E_{ug}$), plus the overcast or clear sky illuminance ($E_{kg}$) on the ground, make up the total horizontal illuminance on the ground surface ($E_{sg}$). A fraction of the ground surface illuminance is then considered diffusely reflected onto the vertical window surface ($E_{gw}$), where *gw* indicates from the ground to the window.

The horizontal ground illuminances can be determined using Figure 7.14, where the clear sky plus sun case and the overcast sky case are functions of solar altitude. The fractions of the ground illuminance diffusely reflected onto the window depend on the reflectivity ($\rho$) of the ground surface (see Table 7.2) and the window-to-ground surface geometry.

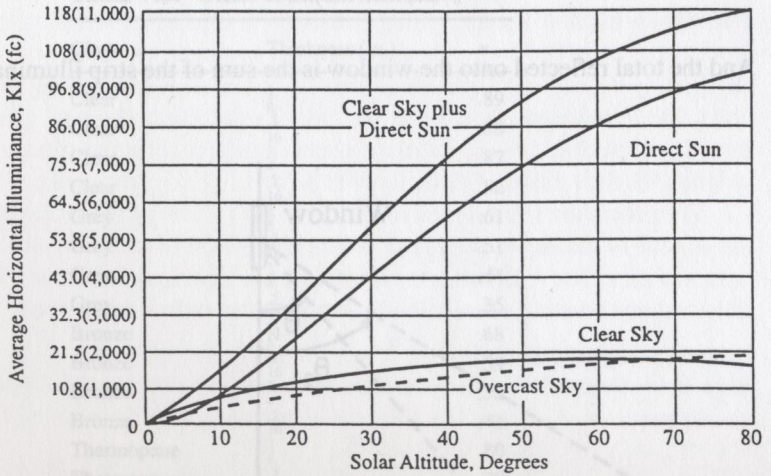


**Figure 7.14.** Horizontal illuminance for overcast sky, clear sky, direct sun, and clear sky plus direct sun. *Source:* Murdoch [23].

**Table 7.2. Ground reflectivities**

| Material | $\rho$ |
|---|---|
| Cement | .27 |
| Concrete | .20–.40 |
| Asphalt | .07–.14 |
| Earth | .10 |
| Grass | .06–.20 |
| Vegetation | .25 |
| Snow | .70 |
| Red brick | .30 |
| Gravel | .15 |
| White paint | .55–.75 |

Murdoch [23].

If the ground surface is considered uniformly reflective from the window outward to the horizon, then the illuminance on the window from ground reflection is

$$E_{gw} = \frac{\rho E_{sg}}{2}. \tag{7.26}$$

A more complicated ground-reflection case is illustrated in Figure 7.15, with multiple strips of differently reflecting ground being handled using the angles to the window, where a strip's illuminance on a window is calculated,

$$E_{gw(\text{strip})} = \frac{\rho_{\text{strip}} E_{sg}}{2}(\cos\theta_1 - \cos\theta_2). \tag{7.27}$$

And the total reflected onto the window is the sum of the strip illuminances:

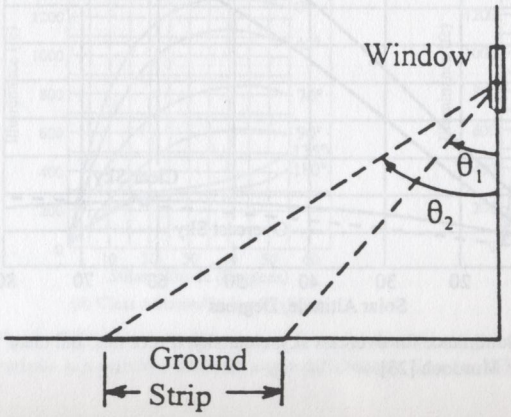


**Figure 7.15.** Geometry for ground strips. *Source:* Murdoch [22].



$$E_{gw} = \frac{E_{sg}}{2}[\rho_1(\cos\theta_0 - \cos\theta_1) + \rho_2(\cos\theta_1 - \cos\theta_2) + \cdots + \rho_n(\cos\theta_{n-1} - \cos 90)]. \tag{7.28}$$

**Step 3: Luminous flux entering space.** The direct sky-sun and ground reflected luminous fluxes entering the building are attenuated by the transmissivity of the window. Table 7.3 presents the transmittance fraction ($\tau$) of several window glasses. The fluxes entering the space are calculated from the total sun-sky and the ground reflected illuminances by using the area of the glass, $A_w$

$$\phi_{sw} = E_{sw}\tau A_w, \tag{7.29}$$

$$\phi_{gw} = E_{gw}\tau A_w.$$

**Step 4: Light loss factor.** The light loss factor ($K_m$) accounts for the attenuation of luminous flux due to dirt on the window (WDD, window dirt depreciation) and on the room surfaces (RSDD, room surface dirt depreciation). WDD depends on how often the window is cleaned, but a 6-month average for offices is 0.83 and for factories is 0.71 [22].

The RSDD is a more complex calculation involving time between cleanings, the direct-indirect flux distribution, and room proportions. However, for rooms cleaned regularly, RSDD is around 0.94 and for once-a-year-cleaned dirty rooms, the RSDD would be around 0.84.

**Table 7.3. Glass transmittances**

| Glass | Thickness (in.) | $\tau$ |
|---|---|---|
| Clear | $\frac{1}{8}$ | .89 |
| Clear | $\frac{3}{16}$ | .88 |
| Clear | $\frac{1}{4}$ | .87 |
| Clear | $\frac{5}{16}$ | .86 |
| Grey | $\frac{1}{8}$ | .61 |
| Grey | $\frac{3}{16}$ | .51 |
| Grey | $\frac{1}{4}$ | .44 |
| Grey | $\frac{5}{16}$ | .35 |
| Bronze | $\frac{1}{8}$ | .68 |
| Bronze | $\frac{3}{16}$ | .59 |
| Bronze | $\frac{1}{4}$ | .52 |
| Bronze | $\frac{5}{16}$ | .44 |
| Thermopane | $\frac{1}{8}$ | .80 |
| Thermopane | $\frac{3}{16}$ | .79 |
| Thermopane | $\frac{1}{4}$ | .77 |

Murdoch [23].

The light loss factor is the product of the preceding two fractions:

$$K_m = (WDD)\,(RSDD). \tag{7.30}$$

**Step 5: Work-plane illuminances.** As discussed earlier, Figure 7.12 illustrates the location of the work-plane illuminances determined with this lumen method of sidelighting. The three illuminances (max, mid, min) are determined using two coefficients of utilization, the *C* factor and *K* factor. The *C* factor depends on room length and width and wall reflectance. The *K* factor depends on ceiling-floor height, room width, and wall reflectance. Table 7.4 presents *C* and *K* values for the three cases of incoming fluxes: (a) sun plus clear sky, (b) overcast sky, and (c) ground reflected. Assumed ceiling and floor reflectances are given for this last case with no window controls (shades, blinds, overhangs, etc.). These further window control complexities can be found in IES [14], LOF [18], and others. A reflectance of 70 percent represents light-colored walls, and 30 percent represents darker walls.

The work-plane max, mid, and min illuminance are each calculated by adding the sun-sky and ground reflected illuminances, which are given by

$$E_{sp} = \phi_{sw} C_s K_s K_m, \tag{7.31}$$

$$E_{gp} = \phi_{gw} C_g K_g K_m,$$

where the *sp* and *gp* refer to the sky-to-work-plane and ground-to-work-plane illuminances.

### 7.4.5 Lumen Method of Skylighting

The lumen method of skylighting calculates the average illuminance at the interior work plane provided by horizontal skylights mounted on the roof. The procedure for skylighting is generally the same as that described above for sidelighting. As with windows, the illuminance from both overcast sky and clear sky plus sun cases are determined for specific days in different seasons and for different times of the day, and a judgment is then made as to the number and size of skylights and any controls needed.

The procedure is presented in four steps: (1) finding the horizontal illuminance on the outside of the skylight; (2) calculating the effective transmittance through the skylight and its well; (3) figuring the interior space light loss factor and the utilization coefficient; and finally, (4) calculating illuminance on the work plane.

**Step 1: Horizontal sky and sun illuminances.** The horizontal illuminance value for an overcast sky or a clear sky plus sun situation can be determined from Figure 7.14 knowing only the solar altitude (see Eq. (2.28)).

**Step 2: Net skylight transmittance.** The transmittance of the skylight is determined by the transmittance of the skylight cover(s), the reflective efficiency of the skylight

**Table 7.4a. C and K factors for no window controls for Overcast Sky**

| Illumination by Overcast Sky<br>C: Coefficient of Utilization | | | | | | | | K: Coefficient of Utilization | | | | | | | | | | | |
|---|---|---|---|---|---|---|---|---|---|---|---|---|---|---|---|---|---|---|---|
| | | 20′ | | 30′ | | 40′ | | | | 8′ | | 10′ | | 12′ | | 14′ | | | |
| Room Length | | | | | | | | | Ceiling Height | | | | | | | | | | |
| Wall Reflectance | | 70% | 30% | 70% | 30% | 70% | 30% | | Wall Reflectance | 70% | 30% | 70% | 30% | 70% | 30% | 70% | 30% | 70% | 30% |
| Room Width | | | | | | | | | Room Width | | | | | | | | | | |
| Max | 20′ | .0276 | .0251 | .0191 | .0173 | .0143 | .0137 | | 20′ | .125 | .129 | .121 | .123 | .111 | .111 | .111 | .111 | .0091 | .0973 |
| | 30′ | .0272 | .0248 | .0188 | .0172 | .0137 | .0131 | Max | 30′ | .122 | .131 | .122 | .121 | .111 | .111 | .111 | .111 | .0945 | .0973 |
| | 40′ | .0269 | .0246 | .0182 | .0171 | .0133 | .0130 | | 40′ | .145 | .133 | .131 | .126 | .111 | .111 | .111 | .111 | .0973 | .0982 |
| Mid | 20′ | .0159 | .0177 | .0101 | .0087 | .0081 | .0071 | | 20′ | .0908 | .0982 | .107 | .115 | .111 | .111 | .111 | .111 | .105 | .122 |
| | 30′ | .0058 | .0050 | .0054 | .0040 | .0034 | .0033 | Mid | 30′ | .156 | .102 | .0939 | .113 | .111 | .111 | .111 | .111 | .121 | .134 |
| | 40′ | .0039 | .0027 | .0030 | .0023 | .0022 | .0019 | | 40′ | .106 | .0948 | .123 | .107 | .111 | .111 | .111 | .111 | .135 | .127 |
| Min | 20′ | .0087 | .0053 | .0063 | .0043 | .0050 | .0037 | | 20′ | .0908 | .102 | .0951 | .114 | .111 | .111 | .111 | .111 | .118 | .134 |
| | 30′ | .0032 | .0019 | .0029 | .0017 | .0020 | .0014 | Min | 30′ | .0924 | .119 | .101 | .114 | .111 | .111 | .111 | .111 | .125 | .126 |
| | 40′ | .0019 | .0009 | .0016 | .0009 | .0012 | .0008 | | 40′ | .111 | .0926 | .125 | .109 | .111 | .111 | .111 | .111 | .133 | .130 |

*Source:* IES, 1979.

## Table 7.4b. C and K factors for no window controls for Clear Sky

Illumination by Clear Sky

C: Coefficient of Utilization

| Room Length | | 20′ | | 30′ | | 40′ | |
|---|---|---|---|---|---|---|---|
| Wall Reflectance | | 70% | 30% | 70% | 30% | 70% | 30% |
| | Room Width | | | | | | |
| Max | 20′ | .0206 | .0173 | .0143 | .0123 | .0110 | .0098 |
| | 30′ | .0203 | .0173 | .0137 | .0120 | .0098 | .0092 |
| | 40′ | .0200 | .0168 | .0131 | .0119 | .0096 | .0091 |
| Mid | 20′ | .0153 | .0104 | .0100 | .0079 | .0083 | .0067 |
| | 30′ | .0082 | .0054 | .0062 | .0043 | .0046 | .0037 |
| | 40′ | .0052 | .0032 | .0040 | .0028 | .0029 | .0023 |
| Min | 20′ | .0106 | .0060 | .0079 | .0049 | .0067 | .0043 |
| | 30′ | .0054 | .0028 | .0047 | .0023 | .0032 | .0021 |
| | 40′ | .0031 | .0014 | .0027 | .0013 | .0021 | .0012 |

K: Coefficient of Utilization

| Ceiling Height | | 8′ | | 10′ | | 12′ | | 14′ | |
|---|---|---|---|---|---|---|---|---|---|
| Wall Reflectance | | 70% | 30% | 70% | 30% | 70% | 30% | 70% | 30% |
| | Room Width | | | | | | | | |
| Max | 20′ | .145 | .155 | .129 | .132 | .111 | .111 | .101 | .0982 |
| | 30′ | .141 | .149 | .125 | .130 | .111 | .111 | .0954 | .101 |
| | 40′ | .157 | .157 | .135 | .134 | .111 | .111 | .0964 | .0991 |
| Mid | 20′ | .110 | .128 | .116 | .126 | .111 | .111 | .103 | .108 |
| | 30′ | .106 | .125 | .110 | .129 | .111 | .111 | .112 | .120 |
| | 40′ | .117 | .118 | .122 | .118 | .111 | .111 | .123 | .122 |
| Min | 20′ | .105 | .129 | .112 | .130 | .111 | .111 | .111 | .116 |
| | 30′ | .0994 | .144 | .107 | .126 | .111 | .111 | .107 | .124 |
| | 40′ | .119 | .116 | .130 | .118 | .111 | .111 | .120 | .118 |

*Source:* IES [13].

## Table 7.4c. C and K factors for no window controls for Ground Illumination (Ceiling Reflectance, 80%; Floor Reflectance, 30%)

Ground Illumination

C: Coefficient of Utilization

| Room Length | | 20′ | | 30′ | | 40′ | |
|---|---|---|---|---|---|---|---|
| Wall Reflectance | | 70% | 30% | 70% | 30% | 70% | 30% |
| | Room Width | | | | | | |
| Max | 20′ | .0147 | .0112 | .0102 | .0088 | .0081 | .0071 |
| | 30′ | .0141 | .0012 | .0098 | .0088 | .0077 | .0070 |
| | 40′ | .0137 | .0112 | .0093 | .0086 | .0072 | .0069 |
| Mid | 20′ | .0128 | .0090 | .0094 | .0071 | .0073 | .0060 |
| | 30′ | .0083 | .0057 | .0062 | .0048 | .0050 | .0041 |
| | 40′ | .0055 | .0037 | .0044 | .0033 | .0042 | .0026 |
| Min | 20′ | .0106 | .0071 | .0082 | .0054 | .0067 | .0044 |
| | 30′ | .0051 | .0026 | .0041 | .0023 | .0033 | .0021 |
| | 40′ | .0029 | .0018 | .0026 | .0012 | .0022 | .0011 |

K: Coefficient of Utilization

| Ceiling Height | | 8′ | | 10′ | | 12′ | | 14′ | |
|---|---|---|---|---|---|---|---|---|---|
| Wall Reflectance | | 70% | 30% | 70% | 30% | 70% | 30% | 70% | 30% |
| | Room Width | | | | | | | | |
| Max | 20′ | .124 | .206 | .140 | .135 | .111 | .111 | .0909 | .0859 |
| | 30′ | .182 | .188 | .140 | .143 | .111 | .111 | .0918 | .0878 |
| | 40′ | .124 | .182 | .140 | .142 | .111 | .111 | .0936 | .0879 |
| Mid | 20′ | .123 | .145 | .122 | .129 | .111 | .111 | .100 | .0945 |
| | 30′ | .0966 | .104 | .107 | .112 | .111 | .111 | .110 | .105 |
| | 40′ | .0790 | .0786 | .0999 | .106 | .111 | .111 | .118 | .118 |
| Min | 20′ | .0994 | .108 | .110 | .114 | .111 | .111 | .107 | .104 |
| | 30′ | .0816 | .0822 | .0984 | .105 | .111 | .111 | .121 | .116 |
| | 40′ | .0700 | .0656 | .0946 | .0986 | .111 | .111 | .125 | .132 |

*Source:* IES [13].

well, the net-to-gross skylight area, and the transmittance of any light-control devices (lenses, louvers, etc.).

The transmittance for several flat-sheet plastic materials used in skylight domes is presented in Table 7.5. To get the effective dome transmittance ($T_D$) from the flat-plate transmittance ($T_F$) value [1], use

$$T_D = 1.25\,T_F(1.18 - 0.416\,T_F). \tag{7.32}$$

If a double-domed skylight is used, then the single-dome transmittances are combined as follows [24]:

$$T_D = \frac{T_{D_1}T_{D_2}}{T_{D_1}T_{D_2} - T_{D_1}T_{D_2}}. \tag{7.33}$$

If the diffuse and direct transmittances for solar radiation are available for the skylight glazing material, it is possible to follow this procedure and determine diffuse and direct dome transmittances separately. However, this difference is usually not a significant factor in the overall calculations.

The efficiency of the skylight well ($N_w$) is the fraction of the luminous flux from the dome that enters the room from the well. The well index (*WI*) is a geometric index (height, h; length, l; width, w) given by

$$WI = \frac{h(w + l)}{2wl}, \tag{7.34}$$

and *WI* is used with the well-wall reflectance value in Figure 7.16 to determine well efficiency, $N_w$.

With $T_D$ and $N_w$ determined, the net skylight transmittance for the skylight and well is given by:

$$T_n = T_D N_W R_A T_C, \tag{7.35}$$

**Table 7.5. Flat-plate plastic material transmittance for skylights**

| Type | Thickness (in.) | Transmittance |
|---|---|---|
| Transparent | $\frac{1}{8}$–$\frac{3}{16}$ | .92 |
| Dense translucent | $\frac{1}{8}$ | .32 |
| Dense translucent | $\frac{3}{16}$ | .24 |
| Medium translucent | $\frac{1}{8}$ | .56 |
| Medium translucent | $\frac{3}{16}$ | .52 |
| Light translucent | $\frac{1}{8}$ | .72 |
| Light translucent | $\frac{3}{16}$ | .68 |

*Source:* Murdoch [22].



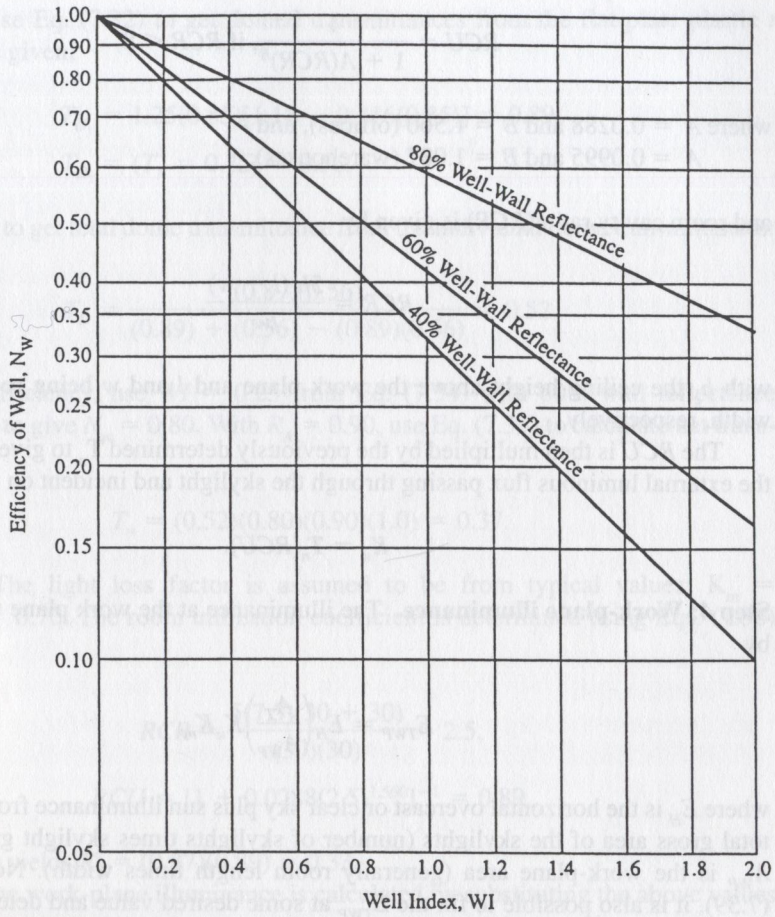


**Figure 7.16.** Efficiency of well versus well index. *Source:* IES [15].

where $R_A$ = ratio of net to gross skylight areas, and $T_C$ = transmittance of any light-controlling devices.

**Step 3: Light loss factor and utilization coefficient.** The light loss factor ($K_m$) is again defined as the product of the room surface direct depreciation (RSDD) and the skylight direct depreciation (SDD) fractions, similarly to Eq. (7.30). Following the reasoning for the sidelighting case, the RSDD value for clean rooms is around 0.94, and 0.84 for dirty rooms. Without specific data indicating otherwise, the SDD fraction is often taken as 0.75 for office buildings and 0.65 for industrial areas.

The fraction of the luminous flux on the skylight that reaches the work plane ($K_u$) is the product of the net transmittance ($T_n$) and the room coefficient of utilization (*RCU*). Dietz et al. [6] developed *RCU* equations for office and warehouse interiors with ceiling, wall, and floor reflectances of 75%, 50%, and 30%, and 50%, 30%, and 20%, respectively.

$$RCU = \frac{1}{1 + A(RCR)^B}, \text{ if } RCR < 8, \tag{7.36}$$

where $A = 0.0288$ and $B = 1.560$ (offices), and
$A = 0.0995$ and $B = 1.087$ (warehouses),

and room cavity ratio ($RCR$) is given by

$$RCR = \frac{5h_c(l + w)}{lw}, \tag{7.37}$$

with $h_c$ the ceiling height above the work plane and $l$ and $w$ being room length and width, respectively.

The $RCU$ is then multiplied by the previously determined $T_n$ to give the fraction of the external luminous flux passing through the skylight and incident on the workplace:

$$K_u = T_n(RCU). \tag{7.38}$$

**Step 4: Work-plane illuminance.** The illuminance at the work plane ($E_{TWP}$) is given by

$$E_{TWP} = E_H\left(\frac{A_T}{A_{WP}}\right)K_u K_m, \tag{7.39}$$

where $E_H$ is the horizontal overcast or clear sky plus sun illuminance from Step 1, $A_T$ is total gross area of the skylights (number of skylights times skylight gross area), and $A_{WP}$ is the work-plane area (generally room length times width). Note that in Eq. (7.39), it is also possible to fix the $E_{TWP}$ at some desired value and determine the skylight area required.

Rules of thumb for skylight placement for uniform illumination include 4 to 8% of roof area and spacing less than 1 1/2 times ceiling-to-work-plane distance between skylights.

**Example 7.5.** Determine the work-plane clear sky plus sun illuminance for a 30′ × 30′ × 10′ office with 75% ceiling, 50% wall, and 30% floor reflectance and with four 4′ × 4′ double-domed skylights at 2 PM on January 15th at 32° latitude. The skylight well is 1′ deep with 60% reflectance walls, and the outer and inner dome flat-plastic transmittances are 0.85 and 0.45, respectively. The net skylight area is 90%.

**Solution.** Follow the four steps in the lumen method for skylighting.

Step 1: Use Figure 7.14 with the solar altitude of 41.7° (calculated from Eq. (2.28)) for the clear sky plus sun curve to get horizontal illuminance:

$$E_H = 7{,}400 \text{ fc}$$



Step 2: Use Eq. (7.32) to get domed transmittances from the flat plate plastic $t$ transmittances given,

$$T_{D_1} = 1.25(0.85)[1.18 - 0.416(0.85)] = 0.89,$$
$$T_{D_2} = (T_F = 0.45) = 0.56,$$

and Eq. (7.33) to get total dome transmittance from the individual dome transmittances:

$$T_D = \frac{(0.89)(0.56)}{(0.89) + (0.56) - (0.89)(0.56)} = 0.52.$$

To get well efficiency, use $WI = 0.25$ from Eq. (7.34) with 60% wall reflectance in Figure 7.16 to give $N_w = 0.80$. With $R_A = 0.90$, use Eq. (7.35) to calculate net transmittance:

$$T_n = (0.52)(0.80)(0.90)(1.0) = 0.37.$$

Step 3: The light loss factor is assumed to be from typical values: $K_m = (0.94)(0.75) = 0.70$. The room utilization coefficient is determined using Eqs. (7.36) and (7.37):

$$RCR = \frac{5(7.5)(30 + 30)}{(30)(30)} = 2.5,$$
$$RCU = [1 + 0.0288(2.5)^{1.560}]^{-1} = 0.89,$$

and Eq. (7.38) yields $K_u = (0.37)(0.89) = 0.33$.

Step 4: The work-plane illuminance is calculated by substituting the above values into Eq. (7.39):

$$E_{TWP} = 7{,}400\left[\frac{4(16)2}{30(30)}\right]0.33(0.70).$$
$$= 122\,fc$$

## PROBLEMS

7.1. Explain how window placement in a building could be defined as: (a) a passive solar feature, (b) an energy conservation technique, and (c) both of the above.

7.2. Write an equation for calculating the cost and savings life-cycle economics of a proposed passive solar system. Explain why it is important to be able to determine the auxiliary energy required for any given passive (or active) system design.

7.3. Referring to the thermal circuit diagram of Figure 7.4 for the thermal storage (Trombe) wall building, construct appropriate thermal circuits for: (a) attached sunspace; (b) thermal storage roof; and (c) direct gain buildings.

7.4. Using rules of thumb for a 200 $m^2$ floor area Denver residence, determine: (a) the auxiliary heating energy required; (b) the solar projected area; and (c) the concrete storage mass needed for a maximum 10°C daily temperature swing.

7.5. A 2000 $ft^2$ house in Boston is being designed with NLC = 12,000 Btu/F-day and 150 $ft^2$ of direct gain. The direct gain system includes double glazing, night-time insulation, and 30 Btu/$ft^2$F thermal storage capacity. Using the LCR method, determine: (a) the annual auxiliary heating energy needed by this design; and (b) the storage mass and dimensions required.

7.6. Compare the annual SSF for 150 $ft^2$ of the following passive systems for the house in Problem 7.5: (a) direct gain (DGA3); (b) vented Trombe wall (TWD4); (c) unvented Trombe wall (TWI4); (d) waterwall (WWB4); and (e) sunspace (SSB4).

7.7. A design modification to the house in Problem 7.5 is desired. A 200 $ft^2$, vented, 12″ thick Trombe wall is to be added to the direct gain system. Assuming the same types of glazing and storage as described above, determine: (a) the annual heating auxiliary energy needed; and (b) the Trombe wall mass.

7.8. Using the SLR method, calculate the auxiliary energy required in March for a 2000 $ft^2$, NLC = 12,000 Btu/F-day, house in Boston with a 150 $ft^2$, night-insulated, double glazed direct gain system with 6″ thick storage floors of 45 Btu/$ft^2$F capacity.

7.9. Calculate the heating season auxiliary energy required for the Boston house in Problem 7.8.

7.10. Determine the length of overhang needed to shade a south-facing 2 m high window in Dallas, TX (latitude 32°51′) to allow for both winter heating and summer shading.

7.11. A 10 mph wind is blowing directly into an open 3 ft × 5 ft window which is mounted in a room's 8 ft high by 12 ft wide wall. If the wind's temperature is 80°F, are the room's occupants thermally comfortable?

7.12. Design a stack effect/solar chimney (vented Trombe wall) to produce an average velocity of 0.3 m/s within a 4 m wide by 5 m long by 3 m high room. Justify your assumptions.

7.13. Estimate the overnight radiant cooling possible from an open, 30°C, 8 m diameter water tank during July in Chicago. What would you expect for convective and evaporative cooling values?

7.14. For the Buried Pipe example (7.4) in the text, determine which of the three flow rate cases leads to the least expensive installation.

7.15. Using Figure 7.9 data, design a 9-ft deep ground-pipe system for Dallas in June to deliver 1000 cfm at 75°F when the outside air temperature is 90°F.

7.16. A 30 ft by 20 ft office space has a photosensor dimmer control working with installed lighting of 2 W/$ft^2$. The required work-place illuminance is 60 fc and the available daylighting is calculated as 40 fc on the summer peak afternoon. Determine the payback period for the dimmer control system assuming the following: 1½ tons cooling installed for 600 $ft^2$ at $2,200/ton; lighting control system cost at $1/$ft^2$; 30% reduction in annual lighting due to daylighting; $0.10/kWh electricity cost; and cooling for 6 months at a $COP_c = 2.5$.



7.17. Determine the illuminances (sun, sky, and ground-reflected) on a vertical, south-facing window at solar noon at 36°N latitude on June 21st and December 21st for: (a) a clear day; and (b) an overcast day.

7.18. Determine the sidelighting work-plane illuminances for a 20 ft long, 15 ft wide (deep), 8 ft high light-colored room with a 15 ft long by 5 ft high window. Assume the direct sun plus clear sky illuminance is 3,000 fc and the ground-reflected illuminance is 200 fc.

7.19. Determine the clear sky day and the cloudy day work-plane illuminances for a 30 ft long, 30 ft wide, 10 ft high light-colored room. A 20 ft long by 7 ft high window with ¼-inch clear glass faces 10°E of South, the building is at 32°N latitude, and it is January 15th at 2 PM solar. The ground outside is covered by dead grass!

7.20. Determine the clear day and cloudy day illuminances on a horizontal skylight at noon on June 21st and December 21st in: (a) Miami; (b) Los Angeles; (c) Denver; (d) Boston; and (e) Seattle.

7.21. A 3 ft by 5 ft double-domed skylight has outer and inner flat-plate plastic transmittances of 0.8 and 0.7, respectively, has a 2 ft deep well with 80% reflectance walls, and has a 90% net skylight area. Calculate the net transmittance of the skylight.

7.22. Determine the number and roof placement of 10 ft by 4 ft skylights needed for a 50 ft by 50 ft by 10 ft high office when the horizontal illuminance is 6,000 fc, the skylight has 45% net transmittance, and the required work-plane illuminance is 100 fc.

7.23. What would be the procedure for producing uniform work-place illuminance when both sidelighting and skylighting are used simultaneously?

## REFERENCES AND SUGGESTED READINGS


1. AAMA. 1977. *Voluntary Standard Procedure for Calculating Skylight Annual Energy Balance.* Chicago, IL: Architectural Aluminum Manufacturers Association Publication. 1602.1.1977.
2. ASES. 1992. *Economics of Solar Energy Technologies.* Eds. R. Larson, F. Vignola, and R. West, American Solar Energy Society, December 1992.
3. ASHRAE. 1989. *Fundamentals: I-P Edition.* Atlanta, GA: American Society of Heating, Refrigerating and Air-Conditioning Engineers.
4. ASHRAE. 1991. *HVAC Applications: I-P Edition.* Atlanta, GA: American Society of Heating, Refrigerating and Air-Conditioning Engineers.
5. Close, D.J., Dunkle, R.V., and Robeson, K.A. 1968. *Design and Performance of a Thermal Storage Air Conditioning System.* Mech. and Eng. Trans., Institute Eng. Australia, MC4, 45.
6. Dietz, P., Murdoch, J., Pokoski, J., and Boyle, J. 1981. "A skylight energy balance analysis procedure." *J. of the Illum. Eng. Soc.* October.
7. Duffie, J.A. and Beckman, W.A. 1991. *Solar Engineering of Thermal Processes.* 2nd Ed., New York: John Wiley and Sons, Inc.
8. Goswami, D.Y. and Dhaliwal, A.S. 1985. Heat transfer analysis in environmental control using an underground air tunnel. *J. of Solar Energy Eng.,* 107 (May): 141–45.
9. Goswami, D.Y. and Ileslamlou, S. 1990. Performance analysis of a closed-loop climate control system using underground air tunnel. *J. of Solar Energy Eng.* 112 (May): 76–81.

10. Goswami, D.Y. and Biseli, K.M. 1994. Use of underground air tunnels for heating and cooling agricultural and residential buildings. Report EES-78, Florida Energy Extension service, University of Florida, Gainesville, Fl. August.
11. Halacy, D.S. 1984. *Home Energy,* Emmaus, PA: Rodale Press, Inc.
12. Hay, H. and Yellot, J. 1969. Natural air conditioning with roof ponds and movable insulation. ASHRAE Transactions 75(1): 165–77.
13. IES. 1979. *Lighting Handbook, Application Volume.* New York: Illumination Engineering Society.
14. Krarti, M. and Kreider, J.F. 1996. Analytical model for heat transfer in an underground air tunnel. Energy Conversion and Management 30(10):1561–74.
15. IES. 1987. *Lighting Handbook, Application Volume.* New York: Illumination Engineering Society.
16. Kusuda, T. and Achenbach, P.R. 1965. Earth temperature and thermal diffusivity at selected stations in the United States. ASHRAE Transactions, 71 (1): 965.
17. Labs, K. 1981. Regional analysis of ground and above ground climate. Report ORNL/Sub-81/40451/1, Oak Ridge National Laboratory, Oak Ridge, TN.
18. LOF. 1976. *How to Predict Interior Daylight Illumination.* Toledo, OH: Libbey-Owens-Ford Co.
19. Marlatt, W., Murray, C. and Squire, S. 1984. Roof pond systems energy technology engineering center. Rockwell International Report No. ETEC 6, April.
20. Martin, M. and Berdahl, P. 1984. Characteristics of infrared sky radiation in the United States, Solar Energy 33(314): 321–36.
21. McQuiston, P.C. and Parker, J.D. 1994. *Heating, Ventilating, and Air Conditioning.* 4th Ed., Wiley, New York.
22. Murdoch, J.B. 1985. *Illumination Engineering: From Edison's Lamp to the Laser.* New York: Macmillan Publishing Co.
23. Olgyay, A. and Olgyay, V. 1967. *Solar Control and Shading Devices.* Princeton, NJ: Princeton University Press.
24. Pierson, O. 1962. *Acrylics for the Architectural Control of Solar Energy.* Philadelphia: Rohm and Haas.
25. PSDH. 1980. *Passive Solar Design Handbook. Volume One: Passive Solar Design Concepts,* DOE/CS-0127/1 March: *Volume Two: Passive Solar Design Analysis,* DOE/CS-0127/2 January. Washington, DC: U.S. Department of Energy.
26. PSDH. 1984. *Passive Solar Design Handbook.* New York: Van Nostrand Reinhold Co.
27. Robbins, C.L. 1986. *Daylighting: Design and Analysis.* New York: Van Nostrand Company, Inc.
28. Rundquist, R.A. 1991. *Daylighting controls: Orphan of HVAC design. ASHRAE J.* November: 30–34.
29. U.S.D.A. 1960. Power to produce. *1960 Yearbook of Agriculture.* U.S. Department of Agriculture.

# SOLAR THERMAL POWER AND PROCESS HEAT

# 8

> The illusion of unlimited powers, nourished by astonishing scientific and technological achievements, has produced the concurrent illusion of having solved the problem of production.
>
> E. F. Schumacher

## 8.1 HISTORICAL PERSPECTIVE

Attempts to harness the sun's energy for power production date back to at least 1774 [56], when the French chemist Lavoisier and the English scientist Joseph Priestley discovered oxygen and developed the theory of combustion by concentrating the rays of the sun on mercuric oxide in a test tube, collecting the gas produced with the aid of solar energy, and burning a candle in the gas. Also, during the same year an impressive picture of Lavoisier was published in which he stands on a platform near the focus of a large glass lens and is carrying out other experiments with focused sunlight (see schematic, Fig. 8.1).

A century later, in 1878, a small solar power plant was exhibited at the World's Fair in Paris (Fig. 8.2). To drive this solar steam engine, sunlight was focused from a parabolic reflector onto a steam boiler located at its focus; this produced the steam that operated a small reciprocating steam engine that ran a printing press. In 1901, a 10-hp solar steam engine was operated by A.G. Eneas in Pasadena, California [6]. It used a 700-ft$^2$ focusing collector the shape of a truncated cone as shown in Fig. 8.3. Between 1907 and 1913 the American engineer F. Shuman developed solar-driven hydraulic pumps; in 1913 he built, jointly with C.V. Boys, a 50-hp solar engine for pumping irrigation water from the Nile near Cairo in Egypt (Fig. 8.4). This device used long parabolic troughs that focused solar radiation onto a central pipe with a concentration ratio of 4.5:1.

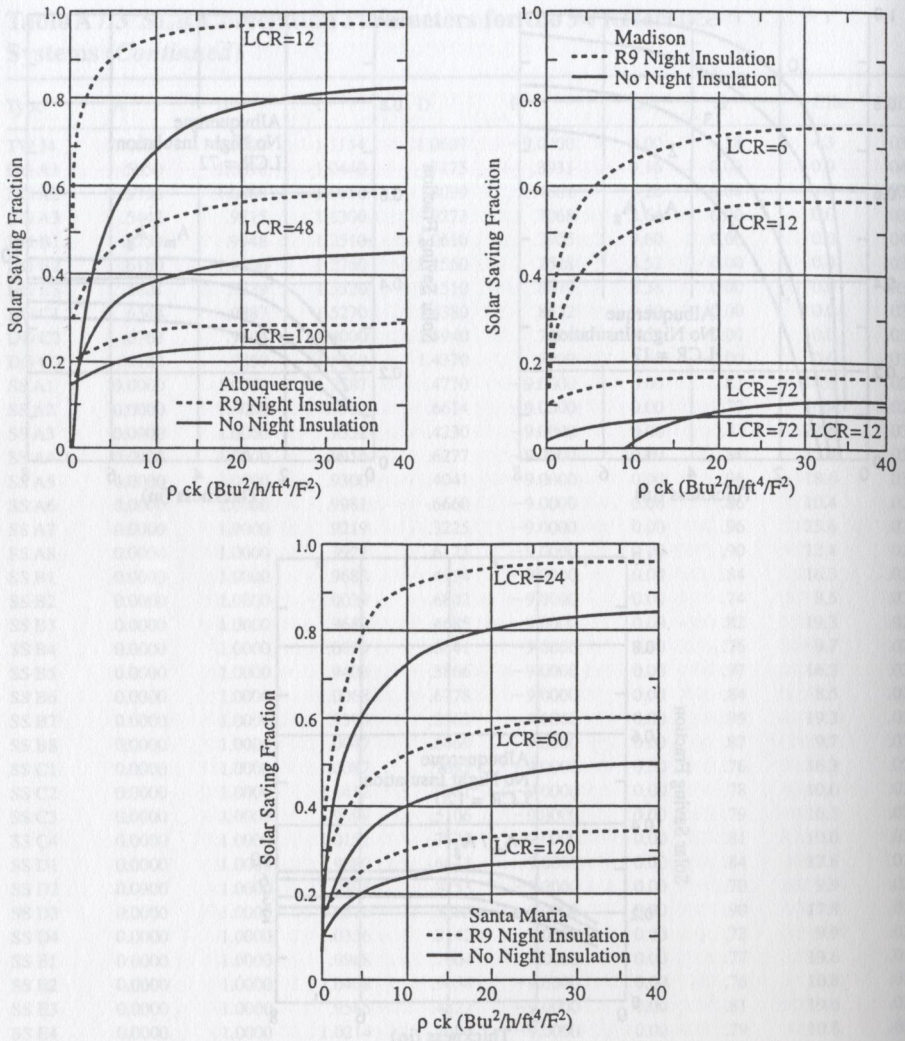


**FIGURE A7.1** (b) Storage Wall: $\rho$ cK Product



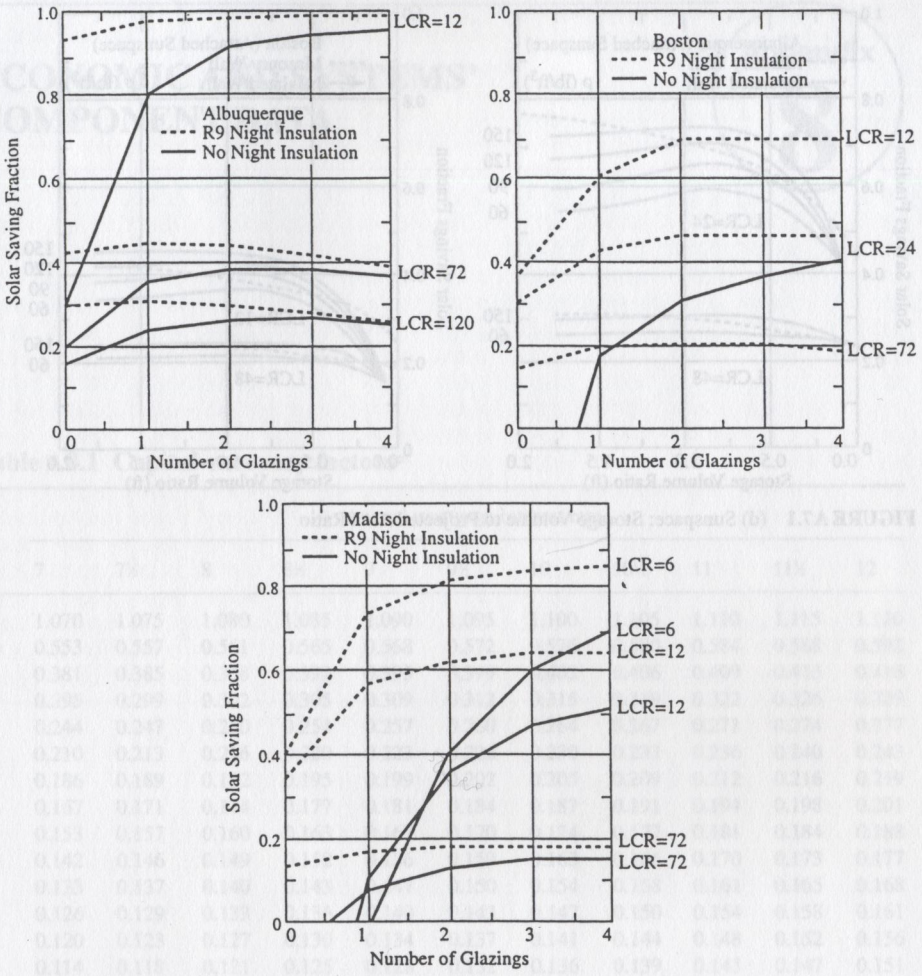


**FIGURE A7.1** (c) Storage Wall: Number of Glazings